© 2014. Published by The Company of Biologists Ltd | Development (2014) 141, 1480-1491 doi:10.1242/dev.098657

RESEARCH ARTICLE

# Vascular endothelial growth factor coordinates islet innervation via vascular scaffolding

**Rachel B. Reinert[1], Qing Cai[1], Ji-Young Hong[2], Jennifer L. Plank[3], Kristie Aamodt[1], Nripesh Prasad[4,5], Radhika Aramandla[2], Chunhua Dai[2], Shawn E. Levy[4], Ambra Pozzi[6,7], Patricia A. Labosky[3], Christopher V. E. Wright[3], Marcela Brissova[2,*] and Alvin C. Powers[1,2,7,*]**

## ABSTRACT

Neurovascular alignment is a common anatomical feature of organs, but the mechanisms leading to this arrangement are incompletely understood. Here, we show that vascular endothelial growth factor (VEGF) signaling profoundly affects both vascularization and innervation of the pancreatic islet. In mature islets, nerves are closely associated with capillaries, but the islet vascularization process during embryonic organogenesis significantly precedes islet innervation. Although a simple neuronal meshwork interconnects the developing islet clusters as they begin to form at E14.5, the substantial ingrowth of nerve fibers into islets occurs postnatally, when islet vascularization is already complete. Using genetic mouse models, we demonstrate that VEGF regulates islet innervation indirectly through its effects on intra-islet endothelial cells. Our data indicate that formation of a VEGF-directed, intra-islet vascular plexus is required for development of islet innervation, and that VEGF-induced islet hypervascularization leads to increased nerve fiber ingrowth. Transcriptome analysis of hypervascularized islets revealed an increased expression of extracellular matrix components and axon guidance molecules, with these transcripts being enriched in the islet-derived endothelial cell population. We propose a mechanism for coordinated neurovascular development within pancreatic islets, in which endocrine cell-derived VEGF directs the patterning of intra-islet capillaries during embryogenesis, forming a scaffold for the postnatal ingrowth of essential autonomic nerve fibers.

**KEY WORDS: VEGF, Endothelial cell, Innervation, Islet, Vascularization**

## INTRODUCTION

Coordinated vascularization and innervation is often a crucial requirement for organogenesis and normal physiological function, but the mechanisms driving these processes during embryonic and postnatal development are far from understood. In many organs, vascular and neural structures are closely aligned (Bearden and Segal, 2005; Correa and Segal, 2012; Mukouyama et al., 2005; Mukouyama et al., 2002; Stubbs et al., 2009), reflecting their interdependent existence (Quaegebeur et al., 2011) and synchronized function (Storkebaum and Carmeliet, 2011). Defining how these vascular and neural elements are patterned is important for a full understanding of organ formation, as well as pathological conditions.

Multiple mechanisms have been proposed to direct neurovascular development. First, vessels and nerves can independently respond to the same signaling factors, including angiogenic factors (VEGF and ephrin families), neurotrophic factors [nerve growth factor (NGF) and glial cell line-derived neurotrophic factor (GDNF) families], and axon guidance molecules (netrins, semaphorins and slits) (reviewed by Carmeliet and Tessier-Lavigne, 2005). For example, large blood vessels and nerves in the developing quail forelimb follow the same semaphorin 3A gradient, without any interdependence between the two structures (Bates et al., 2003). Alternatively, the cells that ultimately form blood vessels (Damon et al., 2007; Honma et al., 2002) and nerve fibers (Mukouyama et al., 2002; Mukouyama et al., 2005) may also release reciprocal guidance cues in a process termed mutual guidance.

The pancreatic islets, miniature endocrine organs that coordinate whole-body glucose homeostasis, are both highly vascularized (Bonner-Weir and Orci, 1982; Brissova et al., 2006; Lammert et al., 2003a) and richly innervated (Ahrén, 2000; Chiu et al., 2012; Rodriguez-Diaz et al., 2011a). Intra-islet capillaries are thicker, denser and more tortuous than capillaries of the exocrine pancreas, and are highly fenestrated (Brissova et al., 2006; Lammert et al., 2003b), allowing for the rapid exchange of nutrients and hormones between the islet and bloodstream. Input from the nervous system fine-tunes islet hormone secretion (Ahrén, 2000), regulates islet blood flow (Atef et al., 1992; Jansson and Hellerström, 1986), and influences β cell mass (Imai et al., 2008; Lausier et al., 2010; Nekrep et al., 2008; Plank et al., 2011). To acquire their specialized vasculature, islet endocrine cells produce angiogenic factors, such as vascular endothelial growth factor A (VEGF), which is crucial for islet vascularization, revascularization and function (Brissova et al., 2006; Cai et al., 2012; Lammert et al., 2003a; Magenheim et al., 2011). Although several recent studies have examined the developmental timing of pancreatic innervation (Burris and Hebrok, 2007; Nekrep et al., 2008; Plank et al., 2011), very little is known about the molecular mechanisms that direct this process, and whether the mechanisms controlling islet vascularization and innervation are interdependent or distinct.

Here, we used genetic mouse models to define the mechanisms that direct neurovascular development within pancreatic islets, with the initial hypothesis that VEGF derived from islet endocrine cells is also a neurotrophic factor. Although formation of the intra-islet vasculature occurs concomitantly with endocrine cell clustering during embryogenesis, the expansion and integration of

[1]Department of Molecular Physiology and Biophysics, Vanderbilt University School of Medicine, Nashville, TN 37232, USA. [2]Division of Diabetes, Endocrinology, and Metabolism, Department of Medicine, Vanderbilt University School of Medicine, Nashville, TN 37232, USA. [3]Department of Cell and Developmental Biology, Vanderbilt University School of Medicine, Nashville, TN 37232, USA. [4]HudsonAlpha Institute for Biotechnology, Huntsville, AL 35806, USA. [5]Department of Biology, University of Alabama-Huntsville, Huntsville, AL 35805, USA. [6]Division of Nephrology and Hypertension, Department of Medicine, Vanderbilt University School of Medicine, Nashville, TN 37232-2372, USA. [7]VA Tennessee Valley Healthcare System, Nashville, TN 37232, USA.

*Authors for correspondence (marcela.brissova@vanderbilt.edu; al.powers@vanderbilt.edu)

**Received 5 June 2013; Accepted 15 January 2014**

Development (2014) doi:10.1242/dev.098657

nerve processes into the islets was significantly delayed until birth, and was completed by the time of weaning. Inactivation of VEGF early in pancreas organogenesis rapidly and dramatically reduced islet vascularization and impaired postnatal nerve fiber ingrowth. By contrast, β cell-specific overexpression of VEGF caused rapid hypervascularization and hyperinnervation of the islet, associated with increased production of extracellular matrix (ECM) components and axon guidance molecules by the intra-islet endothelium. Surprisingly, intra-islet nerves did not express VEGF receptors, but instead were dependent on the VEGF-mediated patterning of the intra-islet vasculature. Collectively, these data demonstrate a new role for VEGF in directing islet innervation.

## RESULTS

### Islet VEGF expression influences islet vascularization and innervation

Although it is well established that adult pancreatic islets are densely vascularized (Brissova et al., 2006; Lammert et al., 2003a) and richly innervated (Ahrén, 2000), little is known about the spatial and temporal relationship of intra-islet capillaries and nerves and the signals guiding their development. To resolve the neurovascular architecture in adult islets, we fluorescently labeled pancreatic sections using markers for nerve fibers (neuronal class III β-tubulin, TUJ1; TUBB3 – Mouse Genome Informatics) and endothelial cells (platelet endothelial cell adhesion molecule 1, PECAM1) (Fig. 1). Confocal microscopy analysis indicated that the majority of TUJ1$^{+}$ fibers was either in a complete or partial alignment with PECAM1$^{+}$ capillaries (Fig. 1A″, closed arrowheads), but some TUJ1$^{+}$ fibers were not adjacent to endothelial cells (Fig. 1A″, open arrowheads). A similar relationship of nerve fibers and intra-islet endothelial cells was confirmed by an additional pan-neuronal marker, synapsin (supplementary material Fig. S1A-A″).

To determine how changes in islet VEGF production affect islet innervation and the relationship of intra-islet capillaries and nerve fibers, we used *Pdx1-Cre;Vegfa*$^{fl/fl}$ (abbreviated VEGF$^{Down}$) mice, in which VEGF is genetically inactivated throughout the pancreas during embryogenesis, resulting in a nearly 90% decrease in islet

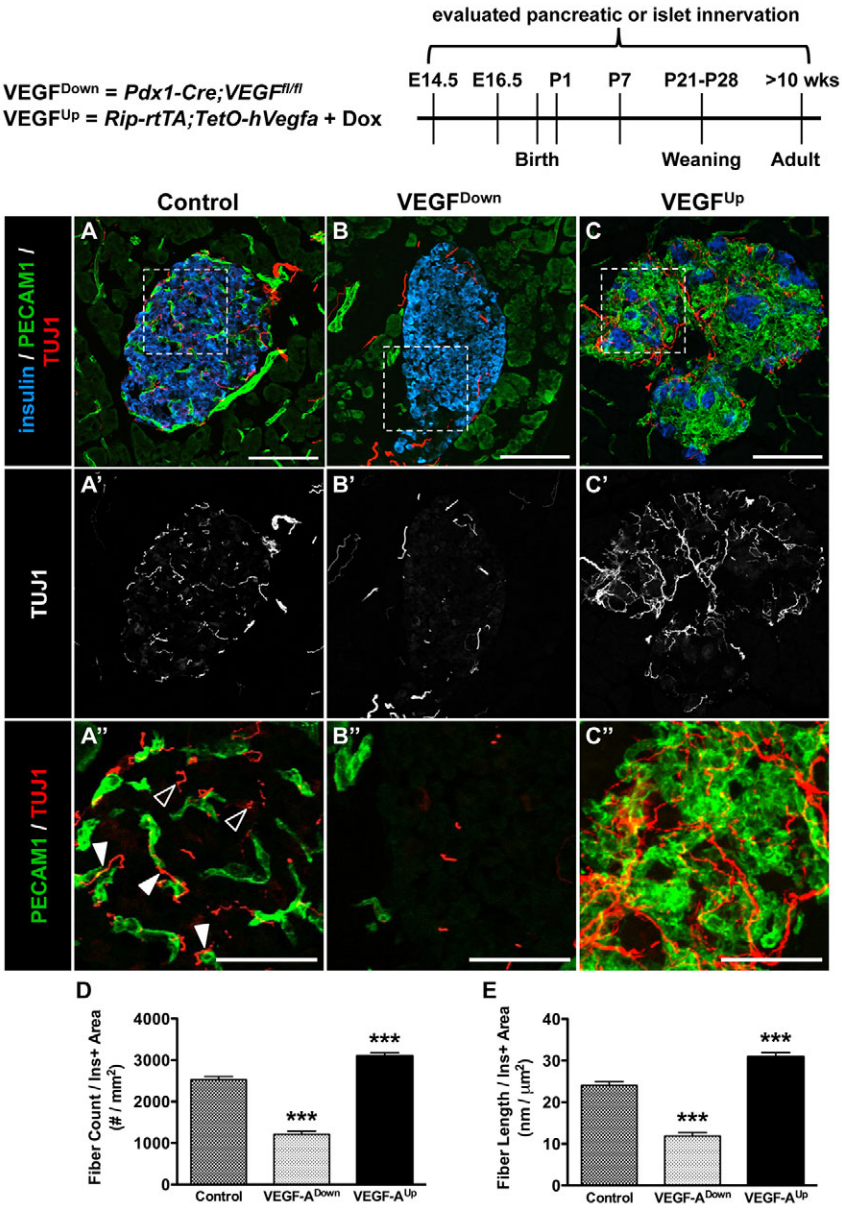


**Fig. 1. Islet innervation follows islet VEGF production and vascularization.** Schematic at the top shows the developmental stages at which pancreatic or islet innervation was examined. (A-C″) Representative islets from adult (>10-week-old) control (A), *Pdx1-Cre;Vegfa*$^{fl/fl}$ (VEGF$^{Down}$; B), and doxycycline-treated (for one week) *RIP-rtTA;TetO-hVegfa* (VEGF$^{Up}$; C) mice, immunolabeled for insulin (blue), PECAM1 (green) and TUJ1 (red). A′-C′ show grayscale images of TUJ1 labeling in A-C. Regions denoted by the dashed line in A, B and C are shown in A″, B″ and C″, respectively. Filled arrowheads point to TUJ1$^{+}$ fibers in a complete or partial alignment with PECAM1$^{+}$ capillaries. Open arrowheads designate TUJ1$^{+}$ fibers that were not adjacent to endothelial cells. (D,E). Morphometric quantification of TUJ1$^{+}$ fiber density (D) and fiber length (E); $n$=4-6 mice per group. Data are summarized as mean ± s.e.m. ***$P$<0.001 versus control group. See also supplementary material Fig. S1. Scale bars: 100 μm (A-C); 50 μm (A″-C″).

Development (2014) doi:10.1242/dev.098657

vascularization (Lammert et al., 2003b; Reinert et al., 2013). To increase islet vascularization, we used a Tet-on inducible system, in which treatment with doxycycline (Dox) induces expression of VEGF in insulin$^+$ β cells (Cai et al., 2012). We treated adult *RIP-rtTA;TetO-hVegfa* (abbreviated VEGF$^{Up}$) mice with Dox for one week, which led to an increase in VEGF secretion, a dramatic expansion of intra-islet endothelial cells, recruitment of macrophages, and a reduction in β cell number (Brissova et al., 2014). Compared with littermate controls (Fig. 1A-A″), islets in adult VEGF$^{Down}$ mice showed reduced innervation (Fig. 1B-B″), as measured by a 52% reduction in the number of TUJ1$^+$ nerve fibers present within the insulin$^+$ area of the islet (Fig. 1D), as well as a 50% reduction in the length of those fibers (Fig. 1E). By contrast, hypervascularized islets in VEGF$^{Up}$ mice were more highly innervated, with nerve fibers more closely associated with endothelial cells than with β cells (Fig. 1C-C″). VEGF-overexpressing islets showed a 23% increase in the number of TUJ1$^+$ nerve fibers (Fig. 1D) and a 29% increase in fiber length (Fig. 1E). The changes in islet innervation in VEGF$^{Down}$ and VEGF$^{Up}$ mice were further confirmed using synapsin labeling (supplementary material Fig. S1). Taken together, these data indicate that the abundance of islet innervation is closely related to the degree of islet vascularization. This suggests that islet innervation may be regulated directly by islet endocrine cell-derived VEGF or signal(s) from intra-islet endothelial cells.

### Both sympathetic and parasympathetic nerve fibers are affected by changes in VEGF expression

Mouse pancreatic islets are primarily innervated by autonomic nerves (Ahrén, 2000; Rodriguez-Diaz et al., 2011a). To determine whether the changes in islet innervation following altered VEGF expression selectively affected sympathetic or parasympathetic nerve fibers, we labeled pancreata from both VEGF$^{Down}$ and VEGF$^{Up}$ mice (and their respective controls) for tyrosine hydroxylase (TH) and vesicular acetylcholine transporter (VAChT).

Control islets contained many TH$^+$ sympathetic nerve fibers and also a few TH-expressing β cells (Fig. 2A). Surprisingly, VEGF$^{Down}$ islets contained few TH$^+$ fibers (Fig. 2B), but the number of TH-expressing β cells dramatically increased. In VEGF-overexpressing islets, TH$^+$ β cells were rare, but these islets had an increased abundance of TH$^+$ fibers (Fig. 2C) compared with controls. VAChT labeling showed that changes in the density of parasympathetic nerve fibers in VEGF$^{Down}$ and VEGF$^{Up}$ islets also coincided with islet VEGF production and islet vascular density (Fig. 2D-F). Regardless of islet VEGF expression, vascularization or innervation status, we did not find evidence of VAChT labeling in islet endocrine cells, in contrast to previous observations in human pancreatic islets (Rodriguez-Diaz et al., 2011b; Rodriguez-Diaz et al., 2011a). These data suggest that islet VEGF expression determines the extent of both islet sympathetic and parasympathetic innervation.

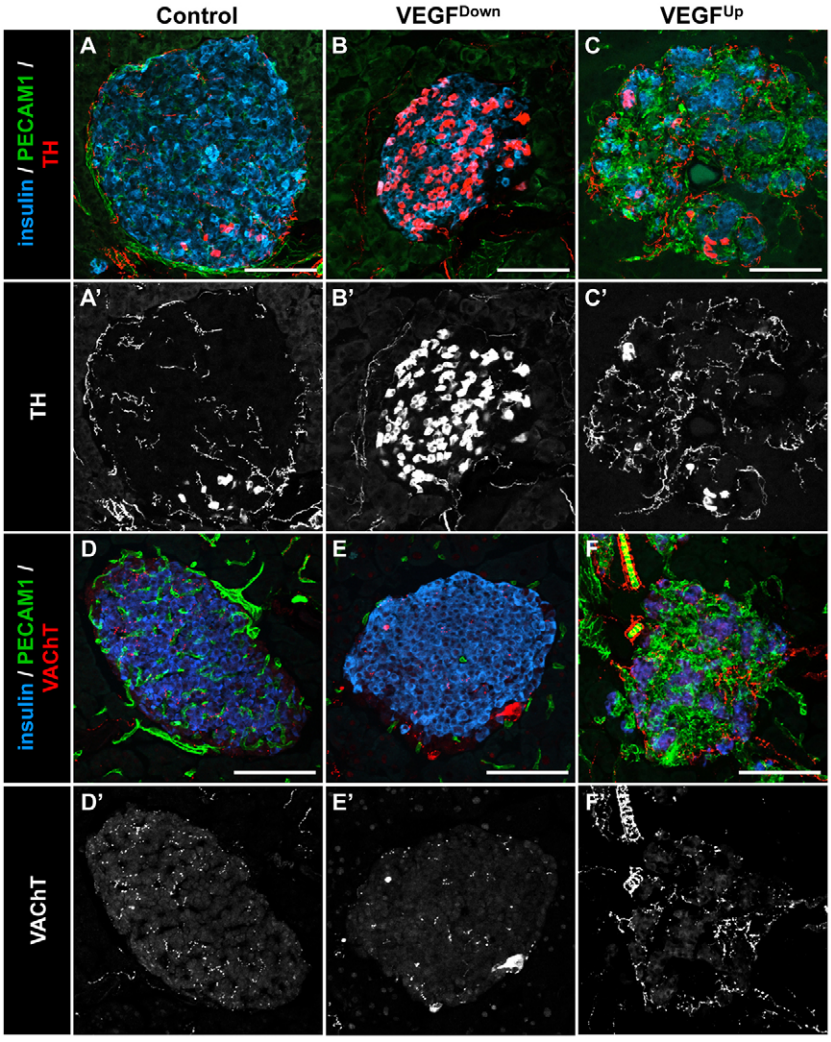


**Fig. 2. Islet VEGF production influences both sympathetic and parasympathetic innervation.** (A-F′) Representative islets from adult (>10-week-old) control (A,D), *Pdx1-Cre;Vegfa$^{fl/fl}$* (VEGF$^{Down}$; B,E), and doxycycline-treated (for one week) *RIP-rtTA;TetO-hVegfa* (VEGF$^{Up}$; C,F) mice, immunolabeled for insulin (blue), PECAM1 (green) and either TH (marker of sympathetic innervation; red in A-C, grayscale in A′-C′) or the vesicular acetylcholine transporter (VAChT; marker of parasympathetic innervation; red in D-F, grayscale in D′-F′). Scale bars: 100 µm.

Development (2014) doi:10.1242/dev.098657

### VEGF is not required for, but enhances, pancreatic innervation during embryogenesis

To follow the establishment of islet innervation and determine when VEGF is important for this process, we assessed several stages throughout pancreas and islet development. Prior lineage-tracing analysis in the *Wnt1-Cre;R26R*$^{YFP/+}$ system demonstrated that neural crest cells enter the pancreatic primordium at approximately embryonic day (E) 10.0, and neuronal processes arrive at developing islets as endocrine cell clusters begin delaminating from the pancreatic epithelium around E13.5 (Plank et al., 2011). However, it is not known when nerve fibers expand into islet clusters and whether this process is coordinated with development of islet vasculature.

Confocal microscopy analysis of whole-mount pancreas at E14.5 revealed that developing islets (visualized by labeling for glucagon$^{+}$ and insulin$^{+}$ endocrine cells) were not only in contact with neural crest derivatives but were also interconnected by the neuronal network traveling between endocrine cell clusters (Fig. 3; supplementary material Movies 1A,B; Fig. S2). This observation brings a new insight into how autonomic nerves may coordinate and synchronize hormone secretion from hundreds of islets dispersed throughout the gland, allowing for oscillations of islet hormone secretion, and optimizing islet hormone secretory output during metabolic stress (Ahrén, 2000). However, nerve fibers remained at the periphery of PDX1$^{high}$-expressing islet clusters at E16.5 (Fig. 4A; supplementary material Movie 3) and E18.5 (supplementary material Fig. S2C).

Global pancreatic inactivation of VEGF in VEGF$^{Down}$ embryos differentially affected the vascular and neuronal tissue compartments. Whereas VEGF loss led to a dramatic reduction in pancreatic vascularization as early as E14.5, the density of TUJ1$^{+}$ neuronal processes and their association with developing endocrine clusters (marked by PDX1$^{high}$ expression) were very similar in mutants and controls (Fig. 4B; supplementary material Movie 4; Fig. S2A-D), indicating that VEGF is not required for the establishment of pancreatic innervation or the migration of nerve processes to developing islets. By contrast, VEGF overexpression by β cells in VEGF$^{Up}$ embryos resulted in greatly increased VEGF production in the vicinity of epithelial tubes (Cai et al., 2012), leading to overall pancreatic hypervascularization (Fig. 4C; supplementary material Movie 5). Three-dimensional reconstructed images of E16.5 pancreata from VEGF$^{Up}$ embryos demonstrated that hypervascularized pancreatic regions were also highly innervated (Fig. 4C; supplementary material Movie 5), suggesting that although VEGF and/or endothelial cells are not required for the development of pancreatic innervation, they greatly enhance and facilitate this process.

As pancreatic innervation in VEGF$^{Down}$ embryos was not affected by reduced pancreatic vascularization, we asked if nerves in the developing pancreas conversely influence vascular development. To answer this question, we used the *Wnt1-Cre;Foxd3*$^{fl/-}$ mouse model to ablate neural crest cells in the pancreas (Plank et al., 2011; Teng et al., 2008). Because these mice die perinatally, we evaluated pancreatic vascularization in embryos at E16.5 (supplementary material Fig. S3A,B). As expected, the pancreatic epithelium in *Wnt1-Cre;Foxd3*$^{fl/-}$ embryos was depleted of TUJ1$^{+}$ nerve fibers (supplementary material Fig. S3B). By contrast, PECAM1$^{+}$ endothelial cells still formed a dense capillary network in *Wnt1-Cre;Foxd3*$^{fl/-}$ embryos, and this was unchanged from controls (supplementary material Fig. S3C). This indicates that neural crest derivatives do not influence pancreatic vascularization. Moreover, these data suggest that the development of pancreatic nerves and blood vessels is guided by different signals.

### Expansion of neuronal processes into islets occurs postnatally and requires VEGF signaling

Given that nerve processes in the embryonic pancreas were still localized at the periphery of developing endocrine clusters at

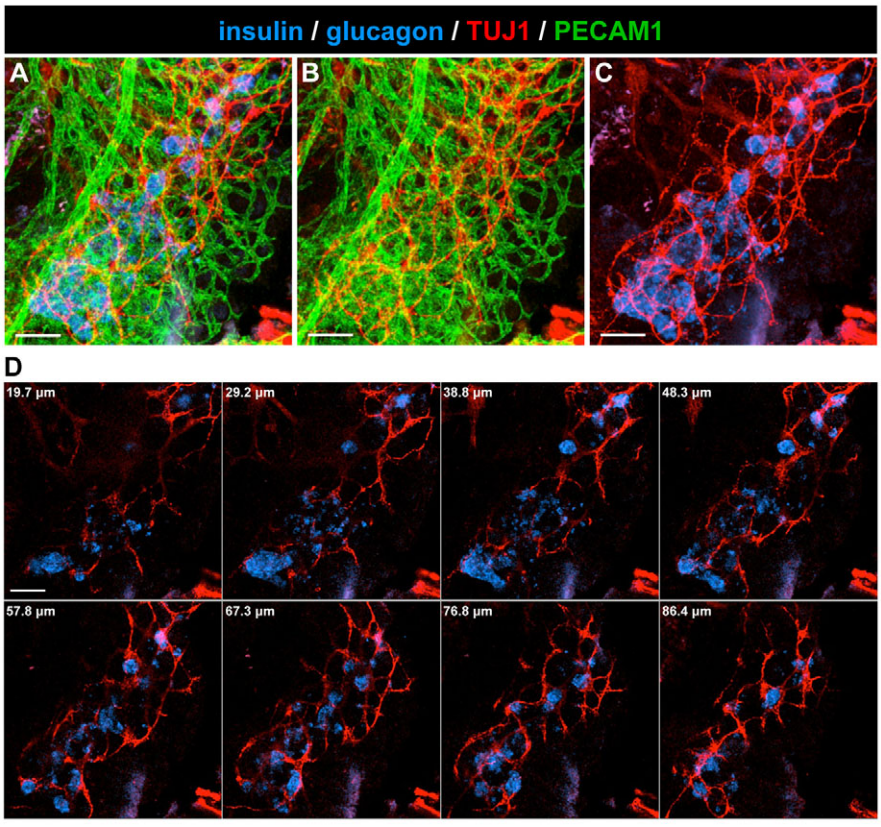


**Fig. 3. Developing islet clusters are interconnected by the neuronal network.** (A-C) Images are 3D reconstructions of a representative confocal *z*-stack (100 µm thick) of E14.5 pancreas from a control mouse, immunolabeled in whole mount. Merge of insulin and glucagon (blue), PECAM1 (green) and TUJ1 (red) labeling is shown in A. The 3D arrangement of blood vessels (PECAM1, green) and nerves (TUJ1, red) is displayed in B. The 3D arrangement of islet clusters (insulin and glucagon, blue) and nerves (TUJ1, red) is shown in C. (D) Single optical slices displaying insulin/glucagon (blue) and TUJ1 (red) labeling from A-C. The optical depth of each slice is indicated in upper left corner. Scale bars: 100 µm. See also supplementary material Movies 1A,B and 2.

Development (2014) doi:10.1242/dev.098657

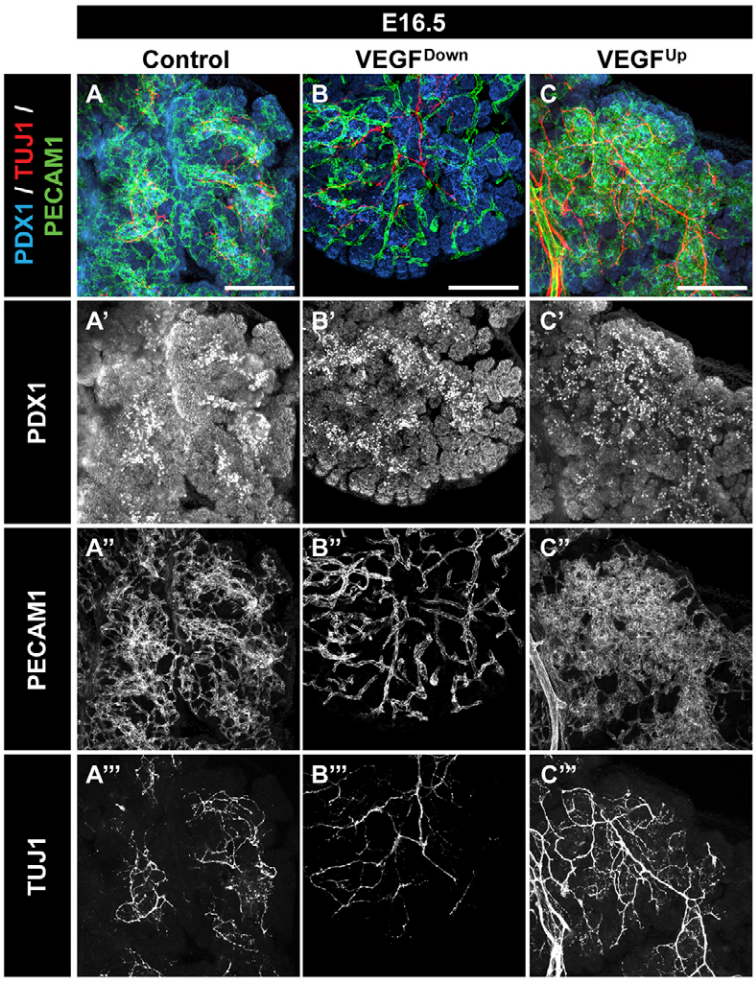


**Fig. 4. VEGF is not required for, but enhances, pancreatic innervation during embryogenesis.** (A-C‴) Images are 3D reconstructions of confocal *z*-stacks (30 µm thick) of E16.5 pancreata from control (A), *Pdx1-Cre;Vegfa*$^{fl/fl}$ (VEGF$^{Down}$; B), and doxycycline-treated (from E5.5) *RIP-rtTA;TetO-hVegfa* (VEGF$^{Up}$; C) mice. Pancreata were immunolabeled in whole mount with antibodies to PDX1 (blue), PECAM1 (green) and TUJ1 (red). (A′-C′) Grayscale images of PDX1 labeling from respective panels A-C. (A″-C″) Grayscale images of PECAM1 labeling from respective panels A-C. (A‴-C‴) Grayscale images of TUJ1 labeling from respective panels A-C. Scale bars: 100 µm (in A-C and corresponding to all panels below). See also supplementary material Figs S2 and S3 and Movies 3-5.

E18.5, we sought to determine the time course of their expansion and integration into islets during postnatal development. At postnatal day (P) 1 and P7, the islet capillary network in controls (Fig. 5A; supplementary material Fig. S4A) resembled that of adult islets, but VEGF$^{Down}$ islets were severely depleted of endothelial cells (Fig. 5B; supplementary material Fig. S4B). Surprisingly, TUJ1$^{+}$ nerve processes continued to be localized at the islet periphery with occasional short projections between peripheral endocrine cells in islets of both genotypes (Fig. 5A,B; supplementary material Fig. S4A,B), indicating that formation of the intra-islet capillary network precedes islet innervation. In control islets, projections of nerve fibers extended into the insulin$^{+}$ core by the time of weaning (P21) (Fig. 5D), but this process was arrested in VEGF$^{Down}$ islets (Fig. 5E). In sharp contrast to control and VEGF$^{Down}$ islets, VEGF$^{Up}$ islets showed a dramatic increase in the number of PECAM1$^{+}$ endothelial cells (Fig. 5C,F; supplementary material Fig. S4C) that disrupted typical β cell clustering owing to greatly increased endothelial cell mass (Cai et al., 2012). However, at each time point, these hypervascularized islets were highly innervated by a dense network of TUJ1$^{+}$ nerve fibers (Figs 5C,F; supplementary material Fig. S4C). These data demonstrate that expansion of neuronal processes into islets occurs postnatally and that normal levels of islet VEGF are crucial for this process.

To further establish when the increase in TH$^{+}$ β cells in hypoinnervated islets is first evident, we examined TH expression at multiple stages of development in VEGF$^{Down}$ mice. At E14.5, E17.5 and P1, few insulin$^{+}$ β cells were TH$^{+}$ in control or VEGF$^{Down}$ mice (supplementary material Fig. S5A-C,F-H). However, TH$^{+}$ β cells became more abundant in VEGF$^{Down}$ islets at P7 (supplementary material Fig. S5D,I) and at P21 (supplementary material Fig. S5E,J), which coincided with the timing when projections of nerve fibers failed to extend into their core (Fig. 5E,E′). By contrast, hypervascularized islets from VEGF$^{Up}$ mice at P7 showed many TH$^{+}$ fibers, but very few β cells expressed TH (supplementary material Fig. S5K). These results show that the number of postnatal β cells expressing TH is inversely correlated with islet innervation.

### Islet neural crest-derived cells do not express VEGF receptors during the postnatal maturation of islet innervation

Because expansion of nerve processes into islets was dynamically controlled by islet VEGF production, we wanted to determine if VEGF directly regulates islet innervation. In cells of the nervous system, VEGF signaling is mediated through VEGF receptor 2 (VEGFR2; KDR – Mouse Genome Informatics) and neuropilin 1 (NRP1). To co-label these receptors with islet neuronal components (nerve fibers and Schwann cells), we used *Wnt1-Cre;R26-EYFP* mice, in which neural crest-derived cells are indelibly labeled with YFP (Plank et al., 2011; Teng et al., 2008). Although both VEGFR2 and NRP1 displayed strong colocalization with PECAM1$^{+}$ capillaries in the islet (Brissova et al., 2006) (data not shown), YFP$^{+}$ neural crest cells did not co-express either

Development (2014) doi:10.1242/dev.098657

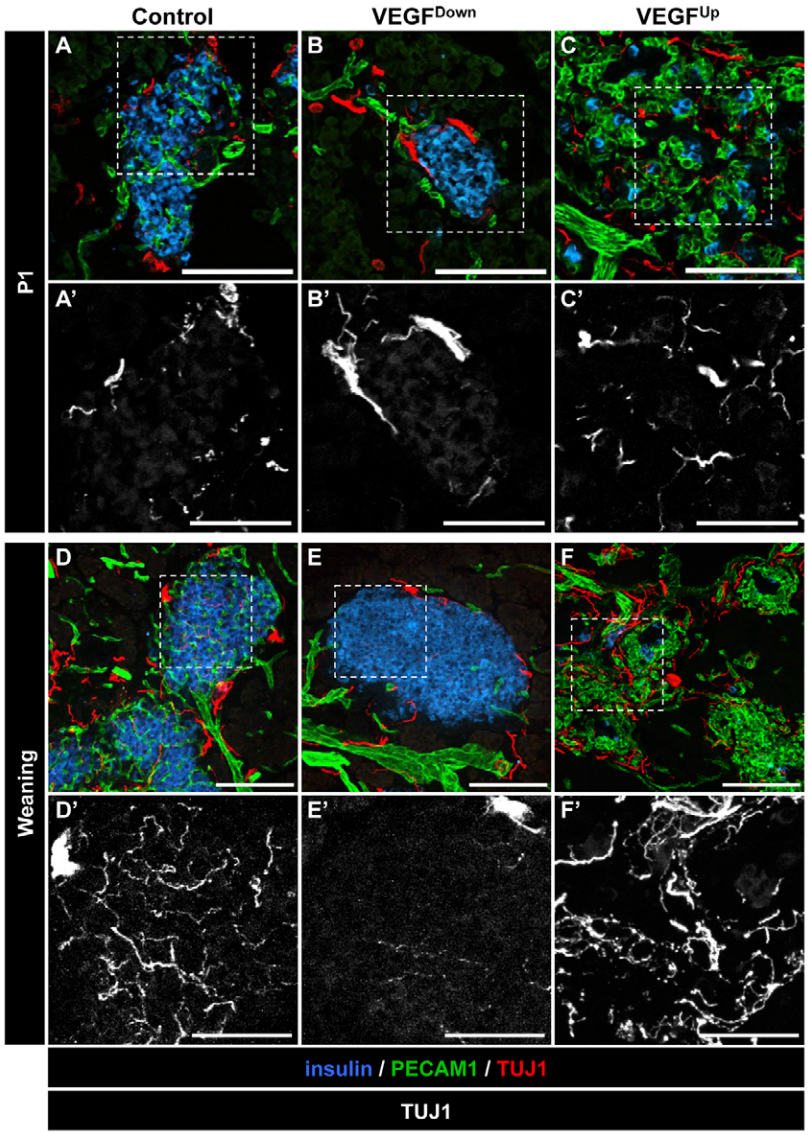


**Fig. 5. Pancreatic islet innervation matures postnatally, and depends on VEGF expression**. (A-F′) Representative islets from control (A,D), *Pdx1-Cre;Vegfa*$^{fl/fl}$ (VEGF$^{Down}$; B,E) and doxycycline-treated (from E5.5) *RIP-rtTA;TetO-hVegfa* (VEGF$^{Up}$; C,F) mice at postnatal day 1 (P1; A-C), and weaning (D-F), immunolabeled for insulin (blue), PECAM1 (green) and TUJ1 (red/grayscale). Regions denoted by the dashed line in A-F are shown in A′-F′, respectively, and display grayscale images of TUJ1 labeling in A-F. Scale bars: 100 µm (A-F); 50 µm (A′-F′). See also supplementary material Figs S4 and S5.

VEGF receptor in adult islets or postnatally, when nerve processes begin to grow into the islets (Fig. 6; supplementary material Fig. S6A-C,E). A few YFP$^{+}$ neural crest cells transiently expressed NRP1, but not VEGFR2, at E16.5 (supplementary material Fig. S6D,F, arrowheads). Therefore, these data indicate that VEGF regulates islet innervation indirectly, through its effects on intra-islet endothelial cells.

### Intra-islet endothelial cells synthesize basement membrane and axon guidance molecules for nerve fiber ingrowth

Because formation of the intra-islet vasculature was crucial for the development of normal islet innervation patterns, and because islet hypervascularization enhanced islet innervation, we reasoned that intra-islet endothelial cells were important mediators of islet neurodevelopment. We hypothesized that intra-islet endothelial cells could act on nerve fibers in two possible ways: by releasing neurotrophic or axon guidance factors and/or by forming a vascular scaffold for migrating nerve fibers. For example, NGF, a signal known to promote sympathetic innervation of the islet (Edwards et al., 1989), may be produced by endothelial cells (Cabrera-Vásquez et al., 2009; Gibran et al., 2003; Tanaka et al., 2004). Alternatively, the ability of a neuron to extend a process over a biological substrate requires a direct interaction with the ECM or basal lamina (Myers et al., 2011).

To identify transcripts of neurotrophic and axon guidance factors, and ECM molecules expressed by intra-islet endothelial cells, we performed transcriptome analyses of control islets, endothelial cell-enriched VEGF$^{Up}$ islets and endothelial cells isolated from VEGF$^{Up}$ islets. We found that members of several classic axon guidance families, such as slits, netrins, semaphorins and ephrins had significantly increased expression in VEGF$^{Up}$ islets (Fig. 7A; supplementary material Table S5), and were highly abundant in the islet endothelial cell fraction (*Slit3*, *Sema3f*, *Sema6d* and *Efnb2*) (Fig. 7B; supplementary material Table S5). Prior studies have shown that, depending on biological context, these molecules may direct either axonal attraction or repulsion (Kolodkin and Tessier-Lavigne, 2011). A few axon guidance molecules that may serve as axon repellents (*Efna5*, *Slitrk6*) were downregulated in VEGF$^{Up}$ islets, together with β cell-specific genes (*Ins2*, *Nkx6-1*, *Pdx1*, *Pax6*) (Fig. 7A), suggesting that these molecules may be β cell-derived.

Surprisingly, intra-islet endothelial cells did not express any known neurotrophic factors (Fig. 7A; supplementary material Table S5). However, we found that *Bdnf* (brain-derived neurotrophic

Development (2014) doi:10.1242/dev.098657

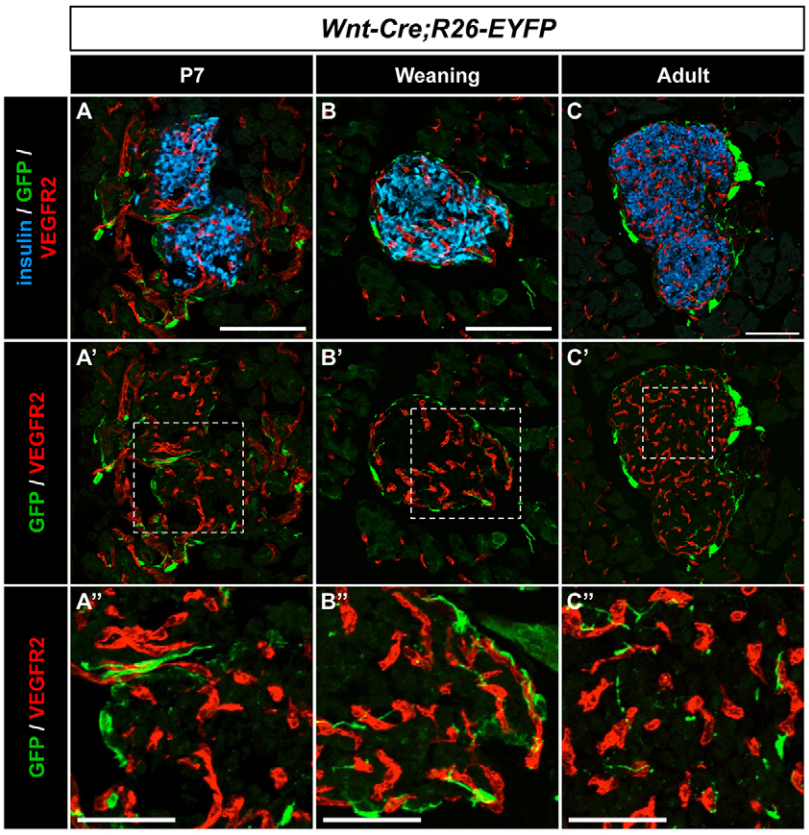


**Fig. 6. Islet neural crest-derived cells do not express VEGF receptors in postnatal life**. Representative islets from *Wnt1-Cre;R26-EYFP* mice at postnatal day 7 (P7; A), weaning (B) and adult (C) stages labeled for insulin (blue), GFP (green) and VEGFR2 (red). Regions denoted by the dashed line in A′, B′ and C′ are shown in A″, B″ and C″, respectively. Scale bars: 100 μm (A-C); 50 μm (A″-C″). See also supplementary material Fig. S6.

factor) expression was appreciably increased in $VEGF^{Up}$ islets and we detected a modest increase in *Ngf* (Fig. 7A; supplementary material Table S5). Because of prior work demonstrating NGF expression in developing islet endocrine and endothelial cells (Cabrera-Vásquez et al., 2009), we also performed quantitative RT-PCR analysis on $VEGF^{Up}$ and $VEGF^{Down}$ islets. *Ngf* expression was increased approximately threefold in $VEGF^{Up}$ islets compared with control (supplementary material Fig. S7A) but was unchanged in endothelial cell-depleted $VEGF^{Down}$ islets (supplementary material Fig. S7B), indicating that NGF is primarily an endocrine cell-derived factor. Furthermore, these data suggest that NGF produced by islet endocrine cells is not sufficient for ingrowth of nerve fibers into islets, and that this process requires intra-islet endothelial cells.

In addition to axon guidance molecules, $VEGF^{Up}$ islets had upregulated expression of several components of the islet basement membrane (Nikolova et al., 2006), including integrins (*Itga1*, *Itga6* and *Itgb1*), collagens (*Col4a1* and *Col4a2*) and laminins (*Lama4*, *Lamb1* and *Lamc1*) all of which were highly expressed in intra-islet endothelial cells (Fig. 7A; supplementary material Fig. S7A; Table S5). Moreover, immunohistochemical analysis showed that intra-islet nerve fibers were closely aligned with endothelial cells expressing collagen IV α1 and laminin during the postnatal period, when nerve fibers begin to penetrate islets, and in adult islets, when innervation is completed (Fig. 7C-D; supplementary material Figs S8-S11). Collectively, these data suggest that intra-islet endothelial cells contribute to islet innervation through synthesis of axon guidance molecules and the vascular basement membrane, which functions as a scaffold for nerve ingrowth.

## DISCUSSION

Vascularization and innervation are crucial for normal organ physiology. Although neurovascular development is often synchronized, diverse mechanisms can achieve this physiologically important ‘goal state’. We elucidated the mechanisms directing neurovascular development in pancreatic islets, the normal function of which depends on dynamic intercommunication between the vascular and nervous systems. By increasing or decreasing local VEGF production during islet development and in mature islets, we showed that: (1) establishment of the intra-islet vasculature by VEGF is essential for the postnatal maturation of islet innervation; (2) intra-islet endothelial cells provide crucial signals for nerves through production of axon guidance molecules and ECM components; and (3) β cells may compensate for a lack of neuronal input via neuro-islet cell plasticity. Therefore, we propose a novel role for VEGF in coordinating neurovascular development within the pancreatic islet. In this organ, VEGF serves as the initial signal in an intra-islet signaling cascade in which endocrine cells establish the vasculature that supports islet endocrine cell development and provides a scaffold for the later ingrowth of nerve fibers to form essential autonomic nervous system connections.

### VEGF is a principal coordinator of islet vascularization and innervation

Both VEGF inactivation and VEGF overexpression within pancreatic islets affected islet innervation. In the VEGF-deficient pancreas, the loss of intra-islet endothelial cells resulted in hypovascularized and hypoinnervated islets. Neural crest-derived cells did associate with these early-stage endocrine cell clusters, but differentiated nerve fibers failed to penetrate the islet core in the postnatal period because of the lack of an established, VEGF-directed intra-islet vascular plexus. Therefore, VEGF-directed formation of the intra-islet vasculature is required for the most essential aspects of final islet innervation. However, the role of

Development (2014) doi:10.1242/dev.098657

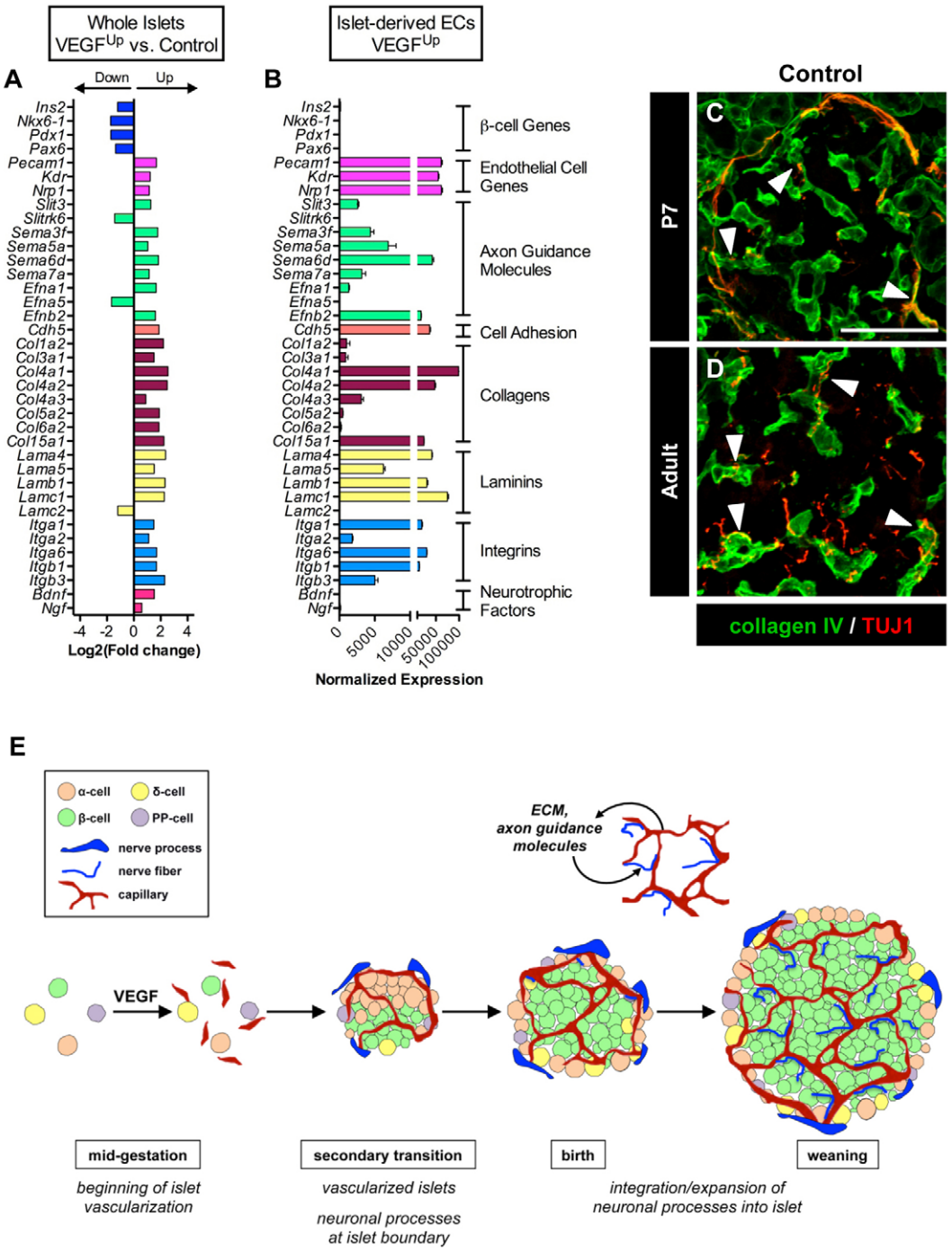


**Fig. 7. Intra-islet endothelial cells modulate islet innervation via synthesis of the vascular basement membrane.** (A) Gene expression profile of whole VEGF$^{Up}$ islets compared with control islets, as determined by RNA-Seq analysis (three replicates/each sample set, $P$<0.05 for fold change ≥2). (B) Transcriptional profile of intra-islet endothelial cells indicates that they synthesize axon guidance molecules and components of the vascular basement membrane. Data are plotted as mean ± s.e.m. See also supplementary material Table S5. (C,D) Pancreatic sections from *Vegfa*$^{fl/fl}$ (Control) mice at P7 (C) and adult (D) stages, immunolabeled for collagen IV (green) and TUJ1 (red). Scale bar: in C, 50 µm for C,D. Arrowheads point to TUJ1$^{+}$ fibers in a complete or partial alignment with collagen IV$^{+}$ capillaries. The corresponding images with insulin labeling are shown in supplementary material Fig. S8A,D. (E) Model of pancreatic islet development. See Discussion for details.

VEGF in islet innervation is indirect, because the neural crest-derived cells did not express the VEGF receptors VEGFR2 or NRP1 at any stage analyzed during the relevant postnatal maturation period. By contrast, islet-specific VEGF overexpression led to dramatic hypervascularization and consequent hyperinnervation.

### Formation of the intra-islet capillary network precedes islet innervation

Our studies show that the recruitment of neural crest-derived cells to the pancreatic bud and the subsequent penetration of nerve fibers into the islet involve distinct stages that are differentially dependent on VEGF and vascularization. We propose a model in which VEGF and

its patterning of islet vascularization direct the final maturation of islet innervation (Fig. 7E). During early organogenesis, endothelial cells are required for induction of the pancreatic buds starting at E8.5 (Lammert et al., 2001). Neural crest-derived cells migrate into the buds between E10.0 and E12.5 (Burris and Hebrok, 2007; Nekrep et al., 2008; Plank et al., 2011; Shimada et al., 2012). VEGF is essential for the initial recruitment of endothelial cells to the developing pancreas, and nascent endocrine cell clusters start to become vascularized and exposed to blood flow as early as E13.5 (Brissova et al., 2006; Shah et al., 2011). Neural crest-derived cells, traveling to the pancreatic anlagen from the foregut (Kirchgessner et al., 1992), associate with early islet clusters independently of VEGF signaling, in part recruited by exocrine pancreas-derived netrin signaling (Jiang et al., 2003). Although differentiated nerves associate with developing islet clusters between E13.5 and E15.5 (Burris and Hebrok, 2007; Nekrep et al., 2008; Plank et al., 2011; Shimada et al., 2012), potentially serving as a broad interconnecting system between the emerging islets, they remain localized at the periphery of vascularized islets at birth. Islet innervation reaches its mature state around the time of weaning, weeks after birth (Burris and Hebrok, 2007), when nerve fibers are finely interspersed within the vascularized islets.

The temporal asynchrony of islet innervation and vascularization fits the proposal that these processes are driven by sequential and independent mechanisms. Additionally, genetic disruption of pancreatic innervation did not affect patterning of the pancreatic vasculature, and did not result in any obvious deterioration of the preformed vascular network. Thus, pancreatic innervation differs from the neurovascular alignment process in limb skin, in which ingrowing peripheral nerves direct arterial differentiation and co-alignment of existing blood vessels through VEGF expression (Mukouyama et al., 2002; Mukouyama et al., 2005). In our model of coordinated islet neurovascular development, endocrine cell- and endothelial cell-derived factors work postnatally to signal nerve fibers to follow capillaries and the endothelial cell-derived vascular basement membrane into the islet core.

### Intra-islet vessels are essential for islet nerve pathfinding

The requirement for vessels in islet innervation is similar to the interdependence seen in the avian gut, wherein the disruption of endothelial cells prevented migration of undifferentiated neural crest cells, ultimately impairing formation of the enteric nervous system (Nagy et al., 2009). In that study, signaling through β1 integrin, a receptor for ECM components, was central to the neural crest-derived cell–endothelial cell interaction. We postulate an analogous interaction in the islet: endothelial cells deposit basement membrane (Nikolova et al., 2006) as a scaffold for traveling nerve fibers.

Islet hypervascularization led to increased production of ECM components and hyperinnervation. These results are similar to a model of inducible angiogenesis in the rat mesentery, in which nerve growth slowly followed the pattern of new vessels, resulting in accurate neurovascular alignment down to the capillary level, though the mechanisms guiding this arrangement were unexplored (Stapor and Murfee, 2012). Transcriptome analysis of hyperinnervated $VEGF^{Up}$ islets demonstrated an increase in the expression of several axon guidance molecules by intra-islet endothelial cells (*Slit3*, *Sema3f*, *Sema6d* and *Efnb2*) which could coordinate resulting neurovascular alignment (Kolodkin and Tessier-Lavigne, 2011). At the same time, decreased expression of β cell-derived axon repellent factors in $VEGF^{Up}$ islets (*Efna5*) due to a concurrent decline in β cell population (marked by decreased expression of β cell genes) could contribute to their increased innervation (Frisén et al., 1998; Kolodkin and Tessier-Lavigne, 2011). Investigation of the role of specific ECM–axon interactions during axon migration into islets will require using mutants with disrupted expression of ECM or integrin molecules. However, these mutant models are not viable at the postnatal stage when the islet innervation takes place (Pöschl et al., 2004; Watt and Hodivala, 1994).

Our data also demonstrate the interesting finding that nerve fibers are closely associated with, yet do not penetrate, pancreatic islets during development and the early postnatal period, despite the presence of an established intra-islet vascular plexus. The reason for this remains unclear. The incomplete alignment of capillaries and nerve endings in adult islets suggests that although intra-islet capillaries form the structural scaffold for nerve fiber migration, endocrine cells are a likely source of neuroattractants that guide the very final stages of innervation, yielding the requisite meshwork of autonomic nervous system connections. Supporting this concept, purified β cells were reported to be more efficient than other islet endocrine cells in promoting reinnervation of islet cell grafts (Myrsén et al., 1996). Alternatively, it is possible that α cells are responsible for producing factors that establish their own neural connections, as the islet periphery is particularly innervated by sympathetic fibers (Chiu et al., 2012; Rodriguez-Diaz et al., 2011a). Islet endocrine and endothelial cells were previously shown to produce NGF throughout development (Cabrera-Vásquez et al., 2009), and experimental overexpression of NGF by β cells led to sympathetic hyperinnervation (Edwards et al., 1989). However, our transcriptome analysis demonstrated that *Ngf* is not produced by intra-islet endothelial cells. Moreover, *Ngf* expression was unchanged in $VEGF^{Down}$ islets, which were depleted of endothelial cells and nerve fibers, indicating that NGF is primarily an endocrine cell-derived factor and is not sufficient for ingrowth of nerve fibers into islets in the absence of intra-islet endothelial cells.

### β cells in hypoinnervated islets may show neuro-islet cell plasticity

VEGF-deficient islets also showed an increased number of β cells expressing TH, normally a marker of catecholaminergic nerves. In control islets, consistent with prior reports (Rodriguez-Diaz et al., 2011a; Teitelman et al., 1988), a small subset of β cells expressed TH. TH expression in β cells has several proposed, yet unconfirmed, roles: (1) a marker of endocrine precursor cells during early pancreas development (Alpert et al., 1988; Teitelman and Lee, 1987; Teitelman et al., 1993); (2) a marker of post-proliferative β cells on the path to senescence (Teitelman et al., 1988); or (3) an indicator of synthesis of endogenous islet catecholamines (Borelli and Gagliardino, 2001; Borelli et al., 2003). The number of $TH^+$ β cells in VEGF-deficient islets begins to increase postnatally, when islet innervation should be reaching its mature state. Thus, we postulate that these hypoinnervated, hypovascularized islets detect a lack of neuronal input, such that some β cells begin to assume the role of catecholamine biosynthesis in compensation. Supporting this hypothesis is the recent observation that genetic ablation of sympathetic nerves during embryonic development leads to a dramatically increased number of $TH^+$ β cells in postnatal islets (Borden et al., 2013). Normal β cells express several other neuronal markers (reviewed in Arntfield and van der Kooy, 2011) and can synthesize neurotransmitters such as dopamine and serotonin (Kim et al., 2010; Ustione and Piston, 2012). Similarly, human α cells express VAChT and produce acetylcholine as a paracrine signal to enhance islet hormone secretion (Rodriguez-Diaz et al., 2011b). Therefore, the increased number of $TH^+$ endocrine cells in VEGF-deficient islets may be an indicator of neuro-islet cell plasticity

(Ahrén et al., 2006), though further work is necessary to test this hypothesis.

### Implications for neurovascular development of human islets

The morphology of human islet innervation has only recently been explored (Rodriguez-Diaz et al., 2011b). Although human islets display fewer nerve fibers than mouse islets, those nerve fibers appear to be more intimately associated with intra-islet capillaries than endocrine cells. It was proposed that this arrangement allows islet neurotransmitters to signal first to arterial smooth muscle cells, thus allowing changes in blood flow to regulate islet function. Alternatively, islet neurotransmitters may be released into the bloodstream before they reach endocrine cells (Rodriguez-Diaz et al., 2011a). Because the close physical relationship between the intra-islet vascular and nervous systems is maintained in human islets, we predict that the vascular-mediated nerve patterning observed in mouse islets is a mechanism that is conserved in humans.

Collectively, our findings emphasize the importance of intercellular signaling networks in organ formation. A detailed understanding of these networks is essential for efforts to develop successful tissue regeneration and transplantation strategies.

## MATERIALS AND METHODS

### Mice

Animal studies were approved by the Institutional Animal Care and Use Committee at Vanderbilt University Medical Center, and were performed in accordance with the Guide for the Care and Use of Laboratory Animals of the National Institutes of Health. For all developmental studies, noon of the date of the observed vaginal plug was considered to be E0.5. Mice were considered adults at 10 weeks of age. Tail biopsies were obtained from all mice for genotyping by PCR using the primers listed (supplementary material Table S1).

For a model of reduced pancreatic VEGF expression (VEGF$^{Down}$), we crossed *Pdx1-Cre* mice (Gu et al., 2002) with mice in which exon 3 of the *Vegfa* gene is flanked by loxP sites (*Vegfa*$^{fl/fl}$) (Gerber et al., 1999). Unless otherwise stated, age-matched *Vegfa*$^{fl/fl}$ mice are shown as controls. For a model of inducible overexpression of VEGF in β cells (VEGF$^{Up}$), we bred *RIP-rtTA* mice (Milo-Landesman et al., 2001) with *TetO-hVegfa*$^{164}$ mice (Ohno-Matsui et al., 2002). To induce VEGF expression, pregnant dams or adult mice were given light-protected drinking water containing 2 mg/ml doxycycline (Dox; Sigma-Aldrich) and 1% Splenda (zero-calorie sucralose sweetener) (Cai et al., 2012). For developmental studies, Dox was administered from E5.5. Adult mice were treated with Dox for 1 week. The Dox solution was freshly prepared every other day.

Neural crest-derived cells were genetically labeled in the pancreas using *Wnt1-Cre* mice (Danielian et al., 1998) crossed with *R26-EYFP* reporter mice (The Jackson Laboratory) (Srinivas et al., 2001). For a model of neural crest cell ablation, *Wnt1-Cre;Foxd3*$^{fl/-}$ embryos were used (Plank et al., 2011; Teng et al., 2008).

### Tissue collection and immunohistochemistry

Postnatal mice and pregnant dams were anesthetized with an intraperitoneal injection of a 90 mg/kg ketamine and 10 mg/kg xylazine solution (Henry Schein) before surgical removal of the pancreas. Pancreata were further dissected and washed in ice-cold 10 mM PBS, fixed in 4% paraformaldehyde in 1× PBS, cryoprotected in 30% w/w sucrose, and frozen in Tissue-Tek Optimal Cutting Temperature (OCT) compound (VWR Scientific Products) before cryosectioning. Cryosections (10-30 µm) were labeled using immunohistochemistry as described previously (Brissova et al., 2004), with the primary and secondary antibodies listed in supplementary material Tables S2 and S3. Slides were mounted with SlowFade Gold antifade reagent (Invitrogen) and sealed with fingernail polish before imaging.

For whole-mount imaging, embryos were dissected in 10 mM PBS to isolate the pancreas, stomach, duodenum and spleen. For each of the following steps, embryonic tissues were placed in cryogenic vials and rocked at 4°C. Tissues were fixed in 4:1 methanol:DMSO overnight, washed twice with 100% methanol, and stored in methanol at −20°C until further use. Before immunolabeling, tissues were rehydrated (washed once in 50% methanol for 30 minutes and twice in 10 mM PBS for 30 minutes each), then blocked and permeabilized in PBSBT (10 mM PBS with 2% bovine serum albumin and 0.5% Triton X-100) in two washes over two hours. On consecutive days, tissues were incubated overnight with primary or secondary antibodies diluted in PBSBT. After each antibody step, tissues were rinsed and washed three to four times with PBSBT for one hour each. Before imaging, immunolabeled tissues were dehydrated (washed once each in 50% and 80% methanol for 30 minutes, and washed twice in 100% methanol over one hour), optically cleared in a 1:2 solution of benzyl alcohol:benzyl benzoate (BABB; Sigma-Aldrich), and placed on a glass coverslip.

Tissue images were obtained using an Olympus BX41 fluorescence microscope, a Leica DMI 6000 B, a Zeiss LSM 510 META laser scanning confocal microscope and a ScanScope FL slide scanner (Aperio Technologies).

### Islet isolation and quantitative RT-PCR

Pancreatic islets were isolated from adult mice as described previously (Brissova et al., 2004), and hand-picked to purity. RNA from 150-400 purified islets (from one to five mice) was extracted as described previously (Dai et al., 2012; Dai et al., 2013). Following extraction, RNA quality and purity was assessed by the Vanderbilt Genome Sciences Resource using a Nanodrop ND-1000 spectrophotometer and an Agilent 2100 Bioanalyzer. Only RNA with a RIN score of >7 was used further.

Quantitative RT-PCR was performed using a TaqMan primer-probe approach, using the primer-probes shown in supplementary material Table S4. Data were analyzed using the $\Delta\Delta C_t$ method (Livak and Schmittgen, 2001), as calculated by the iQ5 system software. Expression of each gene was normalized to *Tbp* (encoding TATA box binding protein) as a reference gene (Dai et al., 2012). The relative expression of *Tbp*-normalized genes in each sample from *Pdx1-Cre;Vegfa*$^{fl/fl}$ mice was compared with each sample of age-matched *Vegfa*$^{fl/fl}$ controls (three to four islet preparations per group), then averaged. Similarly, samples from one-week-Dox-treated *RIP-rtTA;TetO-hVegfa* mice were compared with those from untreated *RIP-rtTA;TetO-hVegfa* controls (four islet preparations per group). Quantitative RT-PCR experiments were performed according to the Minimum Information for Publication of Quantitative Real-Time PCR Experiments (MIQE) guidelines (Bustin et al., 2009).

### Intra-islet endothelial cell isolation and RNA sequencing

Islets were isolated as described previously (Brissova et al., 2004), handpicked in Clonetics EGM MV Microvascular Endothelial Cell Growth Medium (Lonza, Basel, Switzerland), washed three times with 2 mM EDTA/1× PBS, and then dispersed by incubating with Accutase (Innovative Cell Technologies) at 37°C for 10 minutes with constant pipetting. After quenching Accutase with EGM MV media, cells were incubated at 4°C with rat anti-PECAM1-PE antibody (1:500; BD Pharmingen) in FACS buffer (2 mM EDTA/2% fetal bovine serum/1× PBS). Anti-rat Ig, κ CompBead Plus Compensation Particles (BD Biosciences) were used for single color compensation. DAPI (0.25 µg/1,000,000 cells; Invitrogen Molecular Probes) was added to samples for non-viable cell exclusion and cells were sorted using a FACSAria III cell sorter (BD Biosciences). RNA was extracted from whole islets and sorted endothelial cells as described above.

RNA sequencing (RNA-Seq) was performed as described (Brissova et al., 2014). Briefly, RNA from control and VEGF$^{Up}$ islets, and endothelial cells derived from VEGF$^{Up}$ islets (RNAqueous, Ambion) was amplified using a NUGEN Technologies Ovation RNA amplification kit, and sequenced using standard Illumina methods as described (Malone and Oliver, 2011; Mortazavi et al., 2008). Raw sequencing reads were mapped to the mm9 mouse reference genome using TopHat v2.0 (Trapnell et al., 2009). The aligned reads were then imported onto the Avadis NGS data analysis platform (Strand Scientific Intelligence, Bengalor) where they were filtered by their quality metrics. Duplicate reads were then removed and quantification of normalized gene expression was performed using the TMM (trimmed mean of M-values) algorithm (Dillies et al., 2012; Robinson and

Oshlack, 2010). Principal component analysis (PCA) and hierarchal clustering analysis were used to compare the transcriptional profiles from each sample group (control islets, $VEGF^{Up}$ islets, and sorted endothelial cells isolated from $VEGF^{Up}$ islets). Differential expression was calculated based on fold change ≥2.0 and the *P*-value was estimated using *z*-scores (≤0.05) determined by the Benjamini Hochberg false discovery rate (FDR) method (Benjamini and Hochberg, 1995). The RNA-Seq data set from the same biological samples was also used for other studies (Brissova et al., 2014).

### Morphometric analysis and statistics

Quantification of immunohistochemistry was performed on original, unadjusted images with MetaMorph software (Universal Imaging). To represent innervation within islet centers accurately, only islets with a cross-sectional diameter >100 µm were included in the analysis. Morphometric analysis was performed on at least 30 islets per mouse, with $n \geq 4$ mice per group. To assess vascularization in whole mount-labeled *Wnt1-Cre;Foxd3*$^{fl/-}$ embryonic pancreata, vessel density was measured in every other optical section from individual confocal *z*-stacks, totaling >30 slices analyzed per sample (Reinert et al., 2013). Statistics were performed with GraphPad Prism software, using Student's *t*-test or one-way ANOVA to compare groups.

#### Acknowledgements

We thank G. Gu, N. Ferrara, S. Efrat and P. Campochiaro for kindly providing mice. We thank A. L. Kolodkin and R. Brekken for their generous antibody gifts. We thank Greg Poffenberger and Alena Shostak for technical assistance. We are grateful to Maureen Gannon, Danny Winder, Wenbiao Chen, Masakazu Shiota, Elizabeth Blackburn and E. Danielle Dean for their helpful discussions.

#### Competing interests

The authors declare no competing financial interests.

#### Author contributions

R.B.R., M.B., S.E.L., A.P., P.A.L. and A.C.P. conceived and designed the experiments. R.B.R., Q.C., J.-Y.H., J.L.P., K.A., N.P., R.A., C.D. and M.B. performed the experiments. R.B.R., J.L.P., K.A., N.P., C.D., S.E.L., M.B. and A.C.P. analyzed the data. R.B.R., M.B. and A.C.P. wrote the manuscript. R.B.R., K.A., M.B., A.P., P.A.L., C.V.E.W. and A.C.P. reviewed/edited the manuscript.

#### Funding

This work was supported by grants from the Department of Veterans Affairs [BX000666]; the Juvenile Diabetes Research Foundation (JDRF); the National Institutes of Health (NIH) [DK66636, DK69603, DK63439, DK62641, DK72473, DK89572, DK89538, HD36720, R56 DK71052, F30 DK85932 and T32 GM07347]; and the Vanderbilt Diabetes Research and Training Center [DK20593]. Islet isolation was performed in collaboration with the Vanderbilt Islet Procurement and Analysis Core (supported by the Vanderbilt Diabetes Research and Training Center). Image acquisition was performed in part through the use of the Vanderbilt University Medical Center Cell Imaging Shared Resource (supported by NIH grants) [CA68485, DK20593, DK58404, HD15052, DK59637 and EY08126]. Deposited in PMC for release after 12 months.

#### Supplementary material

Supplementary material available online at
http://dev.biologists.org/lookup/suppl/doi:10.1242/dev.098657/-/DC1

#### References

**Ahrén, B.** (2000). Autonomic regulation of islet hormone secretion – implications for health and disease. *Diabetologia* **43**, 393-410.
**Ahrén, B., Wierup, N. and Sundler, F.** (2006). Neuropeptides and the regulation of Islet function. *Diabetes* **55**, S98-S107.
**Alpert, S., Hanahan, D. and Teitelman, G.** (1988). Hybrid insulin genes reveal a developmental lineage for pancreatic endocrine cells and imply a relationship with neurons. *Cell* **53**, 295-308.
**Arntfield, M. E. and van der Kooy, D.** (2011). β-Cell evolution: How the pancreas borrowed from the brain: The shared toolbox of genes expressed by neural and pancreatic endocrine cells may reflect their evolutionary relationship. *Bioessays* **33**, 582-587.
**Atef, N., Ktorza, A., Picon, L. and Pénicaud, L.** (1992). Increased islet blood flow in obese rats: role of the autonomic nervous system. *Am. J. Physiol.* **262**, E736-E740.
**Bates, D., Taylor, G. I., Minichiello, J., Farlie, P., Cichowitz, A., Watson, N., Klagsbrun, M., Mamluk, R. and Newgreen, D. F.** (2003). Neurovascular congruence results from a shared patterning mechanism that utilizes Semaphorin3A and Neuropilin-1. *Dev. Biol.* **255**, 77-98.
**Bearden, S. E. and Segal, S. S.** (2005). Neurovascular alignment in adult mouse skeletal muscles. *Microcirculation* **12**, 161-167.
**Benjamini, Y. and Hochberg, Y.** (1995). A direct approach to false discovery rates. *J. R. Stat. Soc., B* **57**, 289-300.
**Bonner-Weir, S. and Orci, L.** (1982). New perspectives on the microvasculature of the islets of Langerhans in the rat. *Diabetes* **31**, 883-889.
**Borden, P., Houtz, J., Leach, S. D. and Kuruvilla, R.** (2013). Sympathetic innervation during development is necessary for pancreatic islet architecture and functional maturation. *Cell Rep* **4**, 287-301.
**Borelli, M. I. and Gagliardino, J. J.** (2001). Possible modulatory effect of endogenous islet catecholamines on insulin secretion. *BMC Endocr. Disord.* **1**, 1.
**Borelli, M. I., Rubio, M., García, M. E., Flores, L. E. and Gagliardino, J. J.** (2003). Tyrosine hydroxylase activity in the endocrine pancreas: changes induced by short-term dietary manipulation. *BMC Endocr. Disord.* **3**, 2.
**Brissova, M., Fowler, M., Wiebe, P., Shostak, A., Shiota, M., Radhika, A., Lin, P. C., Gannon, M. and Powers, A. C.** (2004). Intraislet endothelial cells contribute to revascularization of transplanted pancreatic islets. *Diabetes* **53**, 1318-1325.
**Brissova, M., Shostak, A., Shiota, M., Wiebe, P. O., Poffenberger, G., Kantz, J., Chen, Z., Carr, C., Jerome, W. G., Chen, J. et al.** (2006). Pancreatic islet production of vascular endothelial growth factor – a is essential for islet vascularization, revascularization, and function. *Diabetes* **55**, 2974-2985.
**Brissova, M., Aamodt, K., Brahmachary, P., Prasad, N., Hong, J.-Y., Dai, C., Mellati, M., Shostak, A., Poffenberger, G., Aramandla, R. et al.** (2014). Islet microenvironment, modulated by vascular endothelial growth factor-A signaling, promotes β cell regeneration. *Cell Metab.* http://dx.doi.org/10.1016/j.cmet.2014.02.001 (in press)
**Burris, R. E. and Hebrok, M.** (2007). Pancreatic innervation in mouse development and beta-cell regeneration. *Neuroscience* **150**, 592-602.
**Bustin, S. A., Benes, V., Garson, J. A., Hellemans, J., Huggett, J., Kubista, M., Mueller, R., Nolan, T., Pfaffl, M. W., Shipley, G. L. et al.** (2009). The MIQE guidelines: minimum information for publication of quantitative real-time PCR experiments. *Clin. Chem.* **55**, 611-622.
**Cabrera-Vásquez, S., Navarro-Tableros, V., Sánchez-Soto, C., Gutiérrez-Ospina, G. and Hiriart, M.** (2009). Remodelling sympathetic innervation in rat pancreatic islets ontogeny. *BMC Dev. Biol.* **9**, 34.
**Cai, Q., Brissova, M., Reinert, R. B., Pan, F. C., Brahmachary, P., Jeansson, M., Shostak, A., Radhika, A., Poffenberger, G., Quaggin, S. E. et al.** (2012). Enhanced expression of VEGF-A in β cells increases endothelial cell number but impairs islet morphogenesis and β cell proliferation. *Dev. Biol.* **367**, 40-54.
**Carmeliet, P. and Tessier-Lavigne, M.** (2005). Common mechanisms of nerve and blood vessel wiring. *Nature* **436**, 193-200.
**Chiu, Y.-C., Hua, T.-E., Fu, Y.-Y., Pasricha, P. J. and Tang, S.-C.** (2012). 3-D imaging and illustration of the perfusive mouse islet sympathetic innervation and its remodelling in injury. *Diabetologia* **55**, 3252-3261.
**Correa, D. and Segal, S. S.** (2012). Neurovascular proximity in the diaphragm muscle of adult mice. *Microcirculation* **19**, 306-315.
**Dai, C., Brissova, M., Hang, Y., Thompson, C., Poffenberger, G., Shostak, A., Chen, Z., Stein, R. and Powers, A. C.** (2012). Islet-enriched gene expression and glucose-induced insulin secretion in human and mouse islets. *Diabetologia* **55**, 707-718.
**Dai, C., Brissova, M., Reinert, R. B., Nyman, L., Liu, E. H., Thompson, C., Shostak, A., Shiota, M., Takahashi, T. and Powers, A. C.** (2013). Pancreatic islet vasculature adapts to insulin resistance through dilation and not angiogenesis. *Diabetes* **62**, 4144-4153.
**Damon, D. H., Teriele, J. A. and Marko, S. B.** (2007). Vascular-derived artemin: a determinant of vascular sympathetic innervation? *Am. J. Physiol.* **293**, H266-H273.
**Danielian, P. S., Muccino, D., Rowitch, D. H., Michael, S. K. and McMahon, A. P.** (1998). Modification of gene activity in mouse embryos in utero by a tamoxifen-inducible form of Cre recombinase. *Curr. Biol.* **8**, 1323-1326.
**Dillies, M.-A., Rau, A., Aubert, J., Hennequet-Antier, C., Jeanmougin, M., Servant, N., Keime, C., Marot, G., Castel, D., Estelle, J. et al.** (2012). A comprehensive evaluation of normalization methods for Illumina high-throughput RNA sequencing data analysis. *Brief Bioinform.* **14**, 671-683.
**Edwards, R. H., Rutter, W. J. and Hanahan, D.** (1989). Directed expression of NGF to pancreatic beta cells in transgenic mice leads to selective hyperinnervation of the islets. *Cell* **58**, 161-170.
**Frisén, J., Yates, P. A., McLaughlin, T., Friedman, G. C., O'Leary, D. D. and Barbacid, M.** (1998). Ephrin-A5 (AL-1/RAGS) is essential for proper retinal axon guidance and topographic mapping in the mammalian visual system. *Neuron* **20**, 235-243.
**Gerber, H. P., Hillan, K. J., Ryan, A. M., Kowalski, J., Keller, G. A., Rangell, L., Wright, B. D., Radtke, F., Aguet, M. and Ferrara, N.** (1999). VEGF is required for growth and survival in neonatal mice. *Development* **126**, 1149-1159.
**Gibran, N. S., Tamura, R., Tsou, R. and Isik, F. F.** (2003). Human dermal microvascular endothelial cells produce nerve growth factor: implications for wound repair. *Shock* **19**, 127-130.
**Gu, G., Dubauskaite, J. and Melton, D. A.** (2002). Direct evidence for the pancreatic lineage: NGN3+ cells are islet progenitors and are distinct from duct progenitors. *Development* **129**, 2447-2457.
**Honma, Y., Araki, T., Gianino, S., Bruce, A., Heuckeroth, R., Johnson, E. and Milbrandt, J.** (2002). Artemin is a vascular-derived neurotropic factor for developing sympathetic neurons. *Neuron* **35**, 267-282.
**Imai, J., Katagiri, H., Yamada, T., Ishigaki, Y., Suzuki, T., Kudo, H., Uno, K., Hasegawa, Y., Gao, J., Kaneko, K. et al.** (2008). Regulation of pancreatic beta cell mass by neuronal signals from the liver. *Science* **322**, 1250-1254.

**Jansson, L. and Hellerström, C.** (1986). Glucose-induced changes in pancreatic islet blood flow mediated by central nervous system. *Am. J. Physiol.* **251**, E644-E647.
**Jiang, Y., Liu, M.-T. and Gershon, M. D.** (2003). Netrins and DCC in the guidance of migrating neural crest-derived cells in the developing bowel and pancreas. *Dev. Biol.* **258**, 364-384.
**Kim, H., Toyofuku, Y., Lynn, F. C., Chak, E., Uchida, T., Mizukami, H., Fujitani, Y., Kawamori, R., Miyatsuka, T., Kosaka, Y. et al.** (2010). Serotonin regulates pancreatic beta cell mass during pregnancy. *Nat. Med.* **16**, 804-808.
**Kirchgessner, A. L., Adlersberg, M. A. and Gershon, M. D.** (1992). Colonization of the developing pancreas by neural precursors from the bowel. *Dev. Dyn.* **194**, 142-154.
**Kolodkin, A. L. and Tessier-Lavigne, M.** (2011). Mechanisms and molecules of neuronal wiring: a primer. *Cold Spring Harb. Perspect. Biol.* **3**, a001727.
**Lammert, E., Cleaver, O. and Melton, D.** (2001). Induction of pancreatic differentiation by signals from blood vessels. *Science* **294**, 564-567.
**Lammert, E., Cleaver, O. and Melton, D.** (2003a). Role of endothelial cells in early pancreas and liver development. *Mech. Dev.* **120**, 59-64.
**Lammert, E., Gu, G., McLaughlin, M., Brown, D., Brekken, R., Murtaugh, L. C., Gerber, H.-P., Ferrara, N. and Melton, D. A.** (2003b). Role of VEGF-A in vascularization of pancreatic islets. *Curr. Biol.* **13**, 1070-1074.
**Lausier, J., Diaz, W. C., Roskens, V., LaRock, K., Herzer, K., Fong, C. G., Latour, M. G., Peshavaria, M. and Jetton, T. L.** (2010). Vagal control of pancreatic ß-cell proliferation. *Am. J. Physiol.* **299**, E786-E793.
**Livak, K. J. and Schmittgen, T. D.** (2001). Analysis of relative gene expression data using real-time quantitative PCR and the 2(-Delta Delta C(T)) Method. *Methods* **25**, 402-408.
**Magenheim, J., Ilovich, O., Lazarus, A., Klochendler, A., Ziv, O., Werman, R., Hija, A., Cleaver, O., Mishani, E., Keshet, E. et al.** (2011). Blood vessels restrain pancreas branching, differentiation and growth. *Development* **138**, 4743-4752.
**Malone, J. H. and Oliver, B.** (2011). Microarrays, deep sequencing and the true measure of the transcriptome. *BMC Biol.* **9**, 34.
**Milo-Landesman, D., Surana, M., Berkovich, I., Compagni, A., Christofori, G., Fleischer, N. and Efrat, S.** (2001). Correction of hyperglycemia in diabetic mice transplanted with reversibly immortalized pancreatic beta cells controlled by the tet-on regulatory system. *Cell Transplant.* **10**, 645-650.
**Mortazavi, A., Williams, B. A., McCue, K., Schaeffer, L. and Wold, B.** (2008). Mapping and quantifying mammalian transcriptomes by RNA-Seq. *Nat. Methods* **5**, 621-628.
**Mukouyama, Y.-S., Shin, D., Britsch, S., Taniguchi, M. and Anderson, D. J.** (2002). Sensory nerves determine the pattern of arterial differentiation and blood vessel branching in the skin. *Cell* **109**, 693-705.
**Mukouyama, Y.-S., Gerber, H.-P., Ferrara, N., Gu, C. and Anderson, D. J.** (2005). Peripheral nerve-derived VEGF promotes arterial differentiation via neuropilin 1-mediated positive feedback. *Development* **132**, 941-952.
**Myers, J. P., Santiago-Medina, M. and Gomez, T. M.** (2011). Regulation of axonal outgrowth and pathfinding by integrin-ECM interactions. *Dev. Neurobiol.* **71**, 901-923.
**Myrsén, U., Keymeulen, B., Pipeleers, D. G. and Sundler, F.** (1996). Beta cells are important for islet innervation: evidence from purified rat islet-cell grafts. *Diabetologia* **39**, 54-59.
**Nagy, N., Mwizerwa, O., Yaniv, K., Carmel, L., Pieretti-Vanmarcke, R., Weinstein, B. M. and Goldstein, A. M.** (2009). Endothelial cells promote migration and proliferation of enteric neural crest cells via beta1 integrin signaling. *Dev. Biol.* **330**, 263-272.
**Nekrep, N., Wang, J., Miyatsuka, T. and German, M. S.** (2008). Signals from the neural crest regulate beta-cell mass in the pancreas. *Development* **135**, 2151-2160.
**Nikolova, G., Jabs, N., Konstantinova, I., Domogatskaya, A., Tryggvason, K., Sorokin, L., Fässler, R., Gu, G., Gerber, H.-P., Ferrara, N. et al.** (2006). The vascular basement membrane: a niche for insulin gene expression and Beta cell proliferation. *Dev. Cell* **10**, 397-405.
**Ohno-Matsui, K., Hirose, A., Yamamoto, S., Saikia, J., Okamoto, N., Gehlbach, P., Duh, E. J., Hackett, S., Chang, M., Bok, D. et al.** (2002). Inducible expression of vascular endothelial growth factor in adult mice causes severe proliferative retinopathy and retinal detachment. *Am. J. Pathol.* **160**, 711-719.
**Plank, J. L., Mundell, N. A., Frist, A. Y., LeGrone, A. W., Kim, T., Musser, M. A., Walter, T. J. and Labosky, P. A.** (2011). Influence and timing of arrival of murine neural crest on pancreatic beta cell development and maturation. *Dev. Biol.* **349**, 321-330.
**Pöschl, E., Schlötzer-Schrehardt, U., Brachvogel, B., Saito, K., Ninomiya, Y. and Mayer, U.** (2004). Collagen IV is essential for basement membrane stability but dispensable for initiation of its assembly during early development. *Development* **131**, 1619-1628.
**Quaegebeur, A., Lange, C. and Carmeliet, P.** (2011). The neurovascular link in health and disease: molecular mechanisms and therapeutic implications. *Neuron* **71**, 406-424.
**Reinert, R. B., Brissova, M., Shostak, A., Pan, F. C., Poffenberger, G., Cai, Q., Hundemer, G. L., Kantz, J., Thompson, C. S., Dai, C. et al.** (2013). Vascular endothelial growth factor-a and islet vascularization are necessary in developing, but not adult, pancreatic islets. *Diabetes* **62**, 4154-4164.
**Robinson, M. D. and Oshlack, A.** (2010). A scaling normalization method for differential expression analysis of RNA-seq data. *Genome Biol.* **11**, R25.
**Rodriguez-Diaz, R., Abdulreda, M. H., Formoso, A. L., Gans, I., Ricordi, C., Berggren, P.-O. and Caicedo, A.** (2011a). Innervation patterns of autonomic axons in the human endocrine pancreas. *Cell Metab.* **14**, 45-54.
**Rodriguez-Diaz, R., Dando, R., Jacques-Silva, M. C., Fachado, A., Molina, J., Abdulreda, M. H., Ricordi, C., Roper, S. D., Berggren, P.-O. and Caicedo, A.** (2011b). Alpha cells secrete acetylcholine as a non-neuronal paracrine signal priming beta cell function in humans. *Nat. Med.* **17**, 888-892.
**Shah, S. R., Esni, F., Jakub, A., Paredes, J., Lath, N., Malek, M., Potoka, D. A., Prasadan, K., Mastroberardino, P. G., Shiota, C. et al.** (2011). Embryonic mouse blood flow and oxygen correlate with early pancreatic differentiation. *Dev. Biol.* **349**, 342-349.
**Shimada, K., Tachibana, T., Fujimoto, K., Sasaki, T. and Okabe, M.** (2012). Temporal and Spatial Cellular Distribution of Neural Crest Derivatives and Alpha Cells during Islet Development. *Acta Histochem. Cytochem.* **45**, 65-75.
**Srinivas, S., Watanabe, T., Lin, C. S., William, C. M., Tanabe, Y., Jessell, T. M. and Costantini, F.** (2001). Cre reporter strains produced by targeted insertion of EYFP and ECFP into the ROSA26 locus. *BMC Dev. Biol.* **1**, 4.
**Stapor, P. C. and Murfee, W. L.** (2012). Spatiotemporal distribution of neurovascular alignment in remodeling adult rat mesentery microvascular networks. *J. Vasc. Res.* **49**, 299-308.
**Storkebaum, E. and Carmeliet, P.** (2011). Paracrine control of vascular innervation in health and disease. *Acta Physiol. (Oxf.)* **203**, 61-86.
**Stubbs, D., DeProto, J., Nie, K., Englund, C., Mahmud, I., Hevner, R. and Molnár, Z.** (2009). Neurovascular congruence during cerebral cortical development. *Cereb. Cortex* **19** Suppl. 1, i32-i41.
**Tanaka, A., Wakita, U., Kambe, N., Iwasaki, T. and Matsuda, H.** (2004). An autocrine function of nerve growth factor for cell cycle regulation of vascular endothelial cells. *Biochem. Biophys. Res. Commun.* **313**, 1009-1014.
**Teitelman, G. and Lee, J. K.** (1987). Cell lineage analysis of pancreatic islet development: glucagon and insulin cells arise from catecholaminergic precursors present in the pancreatic duct. *Dev. Biol.* **121**, 454-466.
**Teitelman, G., Alpert, S. and Hanahan, D.** (1988). Proliferation, senescence, and neoplastic progression of beta cells in hyperplasic pancreatic islets. *Cell* **52**, 97-105.
**Teitelman, G., Alpert, S., Polak, J. M., Martinez, A. and Hanahan, D.** (1993). Precursor cells of mouse endocrine pancreas coexpress insulin, glucagon and the neuronal proteins tyrosine hydroxylase and neuropeptide Y, but not pancreatic polypeptide. *Development* **118**, 1031-1039.
**Teng, L., Mundell, N. A., Frist, A. Y., Wang, Q. and Labosky, P. A.** (2008). Requirement for Foxd3 in the maintenance of neural crest progenitors. *Development* **135**, 1615-1624.
**Trapnell, C., Pachter, L. and Salzberg, S. L.** (2009). TopHat: discovering splice junctions with RNA-Seq. *Bioinformatics* **25**, 1105-1111.
**Ustione, A. and Piston, D. W.** (2012). Dopamine synthesis and D3 receptor activation in pancreatic β-cells regulates insulin secretion and intracellular [Ca(2+)] oscillations. *Mol. Endocrinol.* **26**, 1928-1940.
**Watt, F. M. and Hodivala, K. J.** (1994). Cell adhesion. Fibronectin and integrin knockouts come unstuck. *Curr. Biol.* **4**, 270-272.

**Reinert Fig. S1**

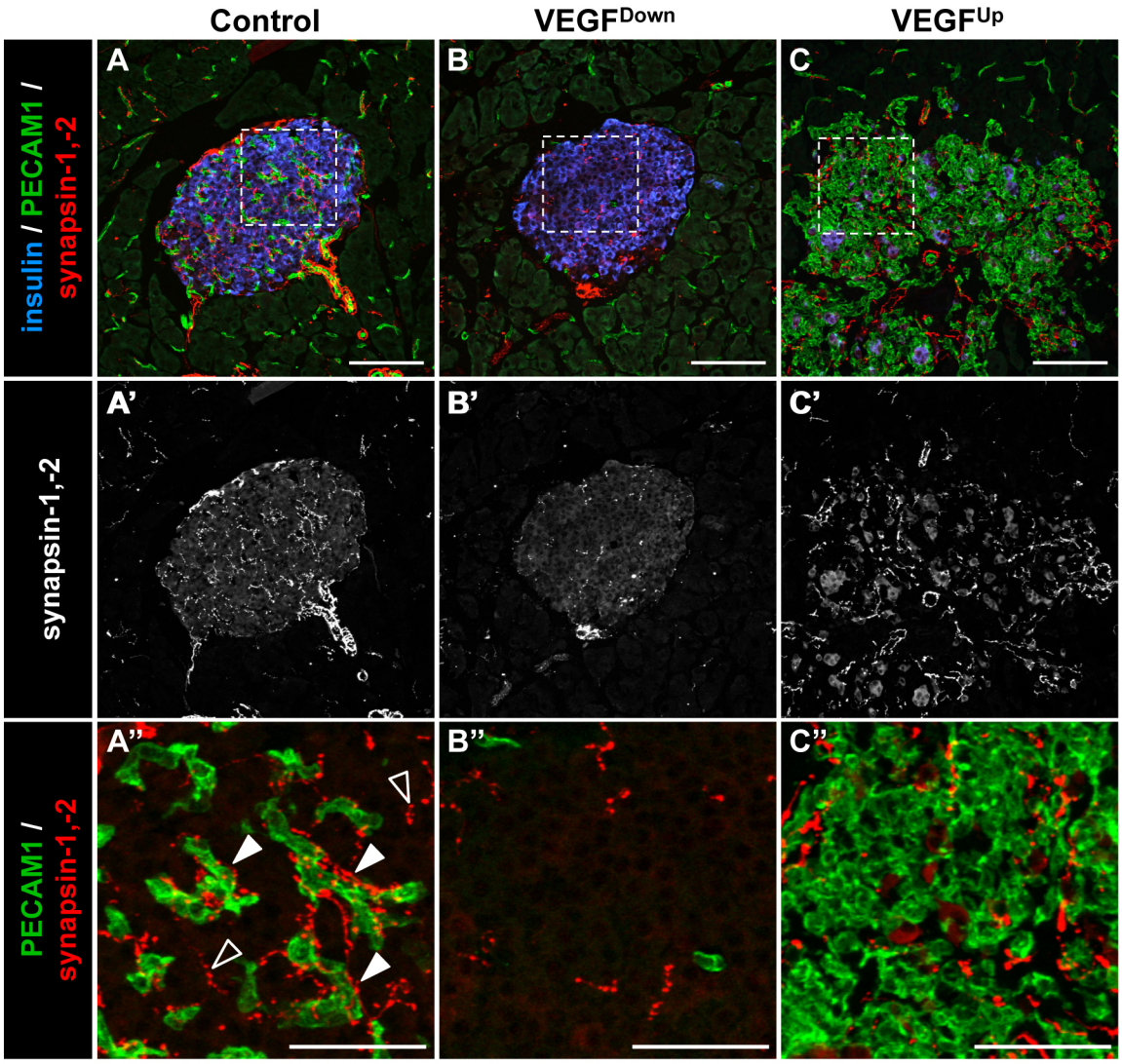

**Reinert Fig. S2**

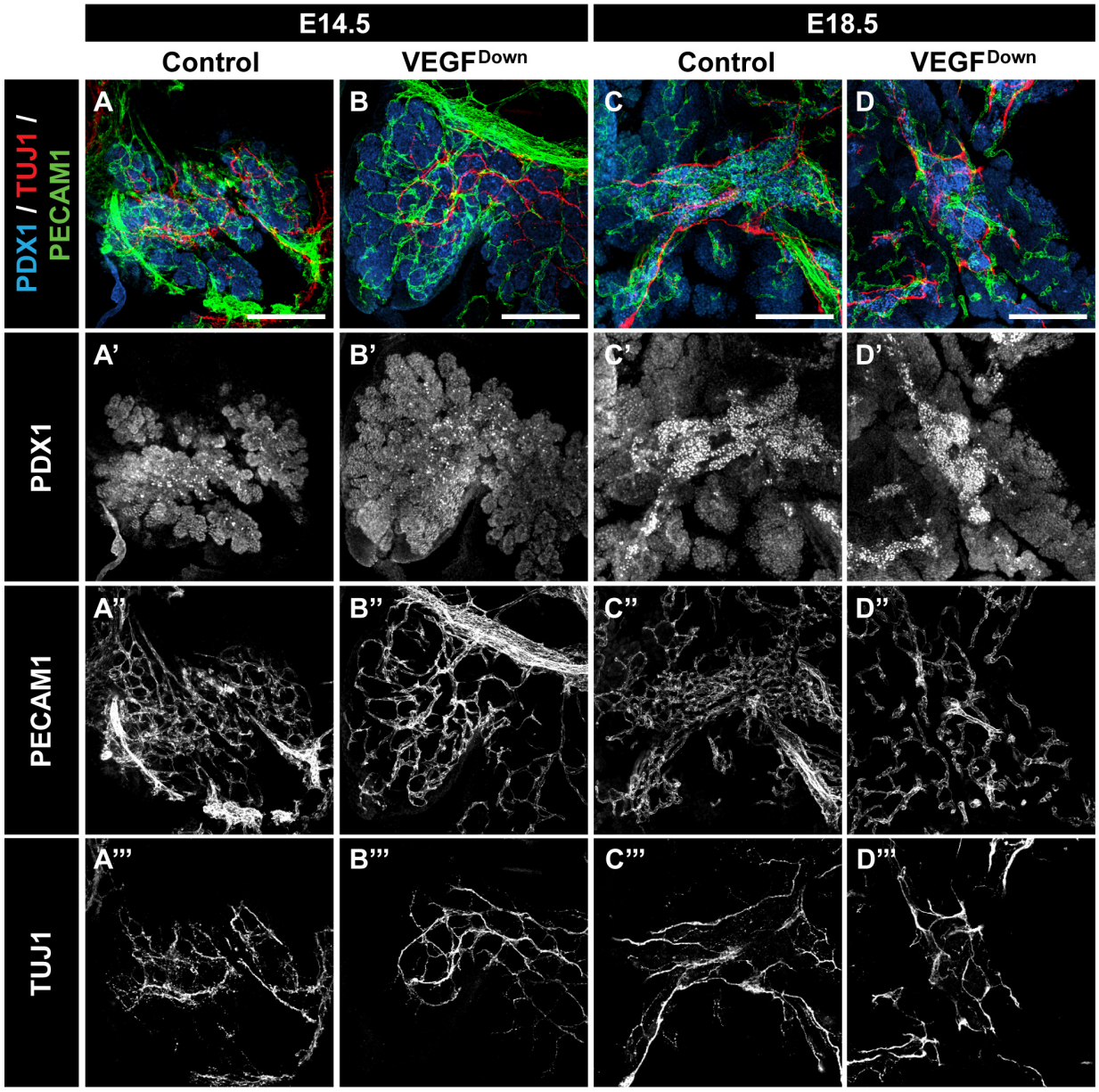

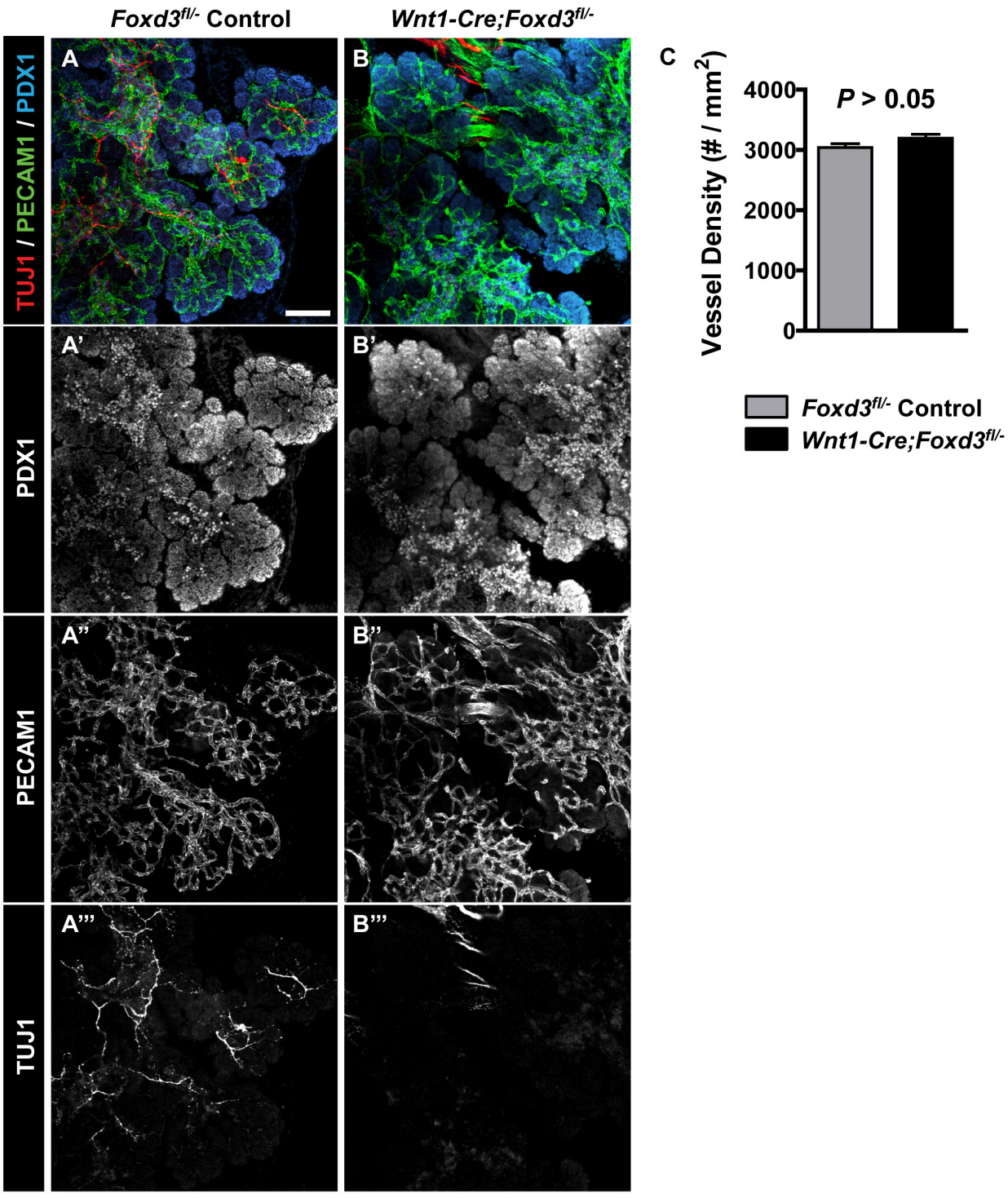
Foxd3fl/- Control
Wnt1-Cre;Foxd3fl/-
TUJ1 / PECAM1 / PDX1
PDX1
PECAM1
TUJ1
A
B
A'
B'
A''
B''
A'''
B'''
C
Vessel Density (# / mm2)
4000
3000
2000
1000
0
P > 0.05
Foxd3fl/- Control
Wnt1-Cre;Foxd3fl/-

**Reinert Fig. S4**

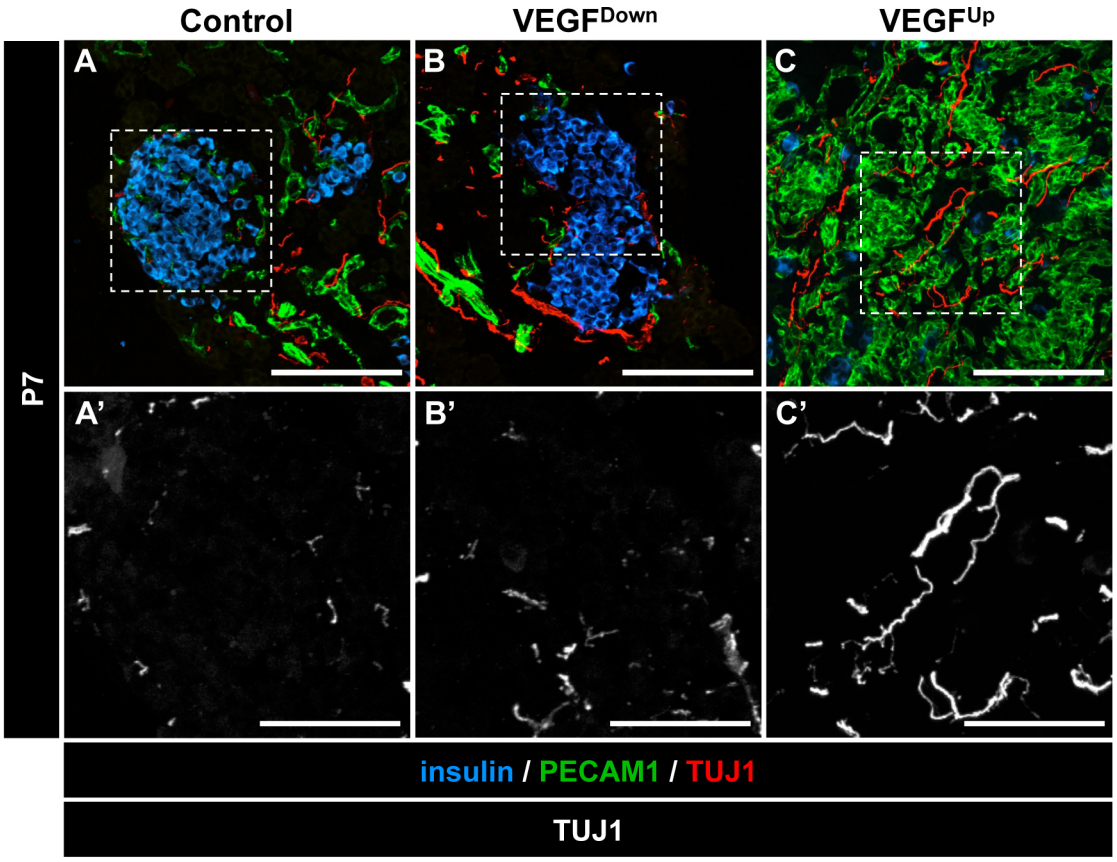

Reinert Fig. S5

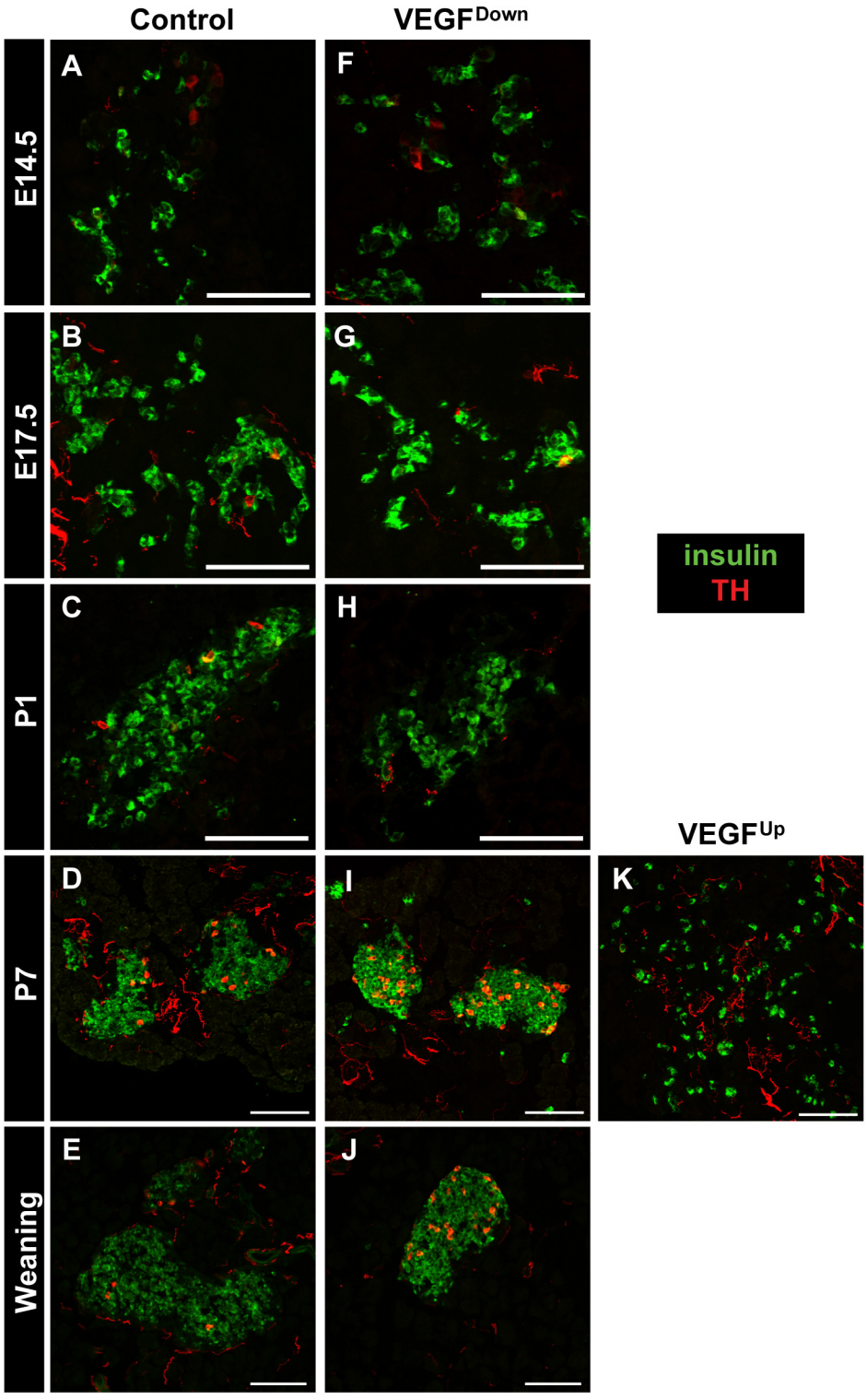

**Reinert Fig. S6**

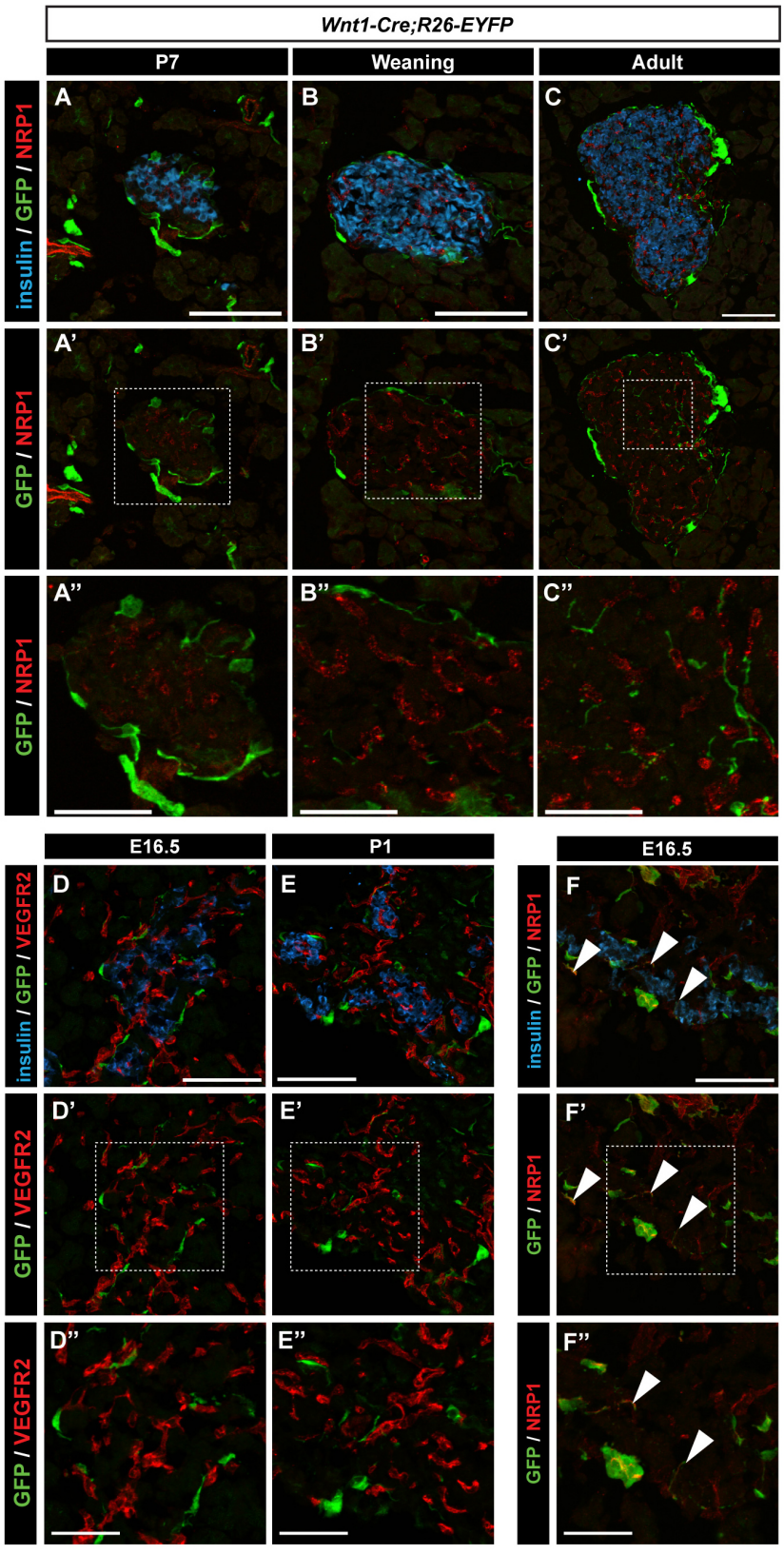

**Reinert Fig. S7**

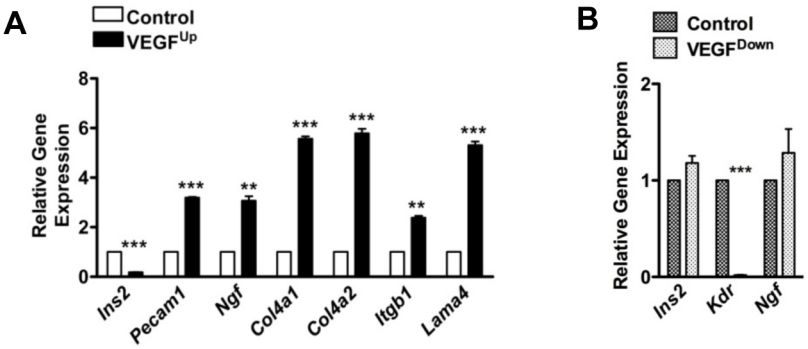

Reinert Fig. S8

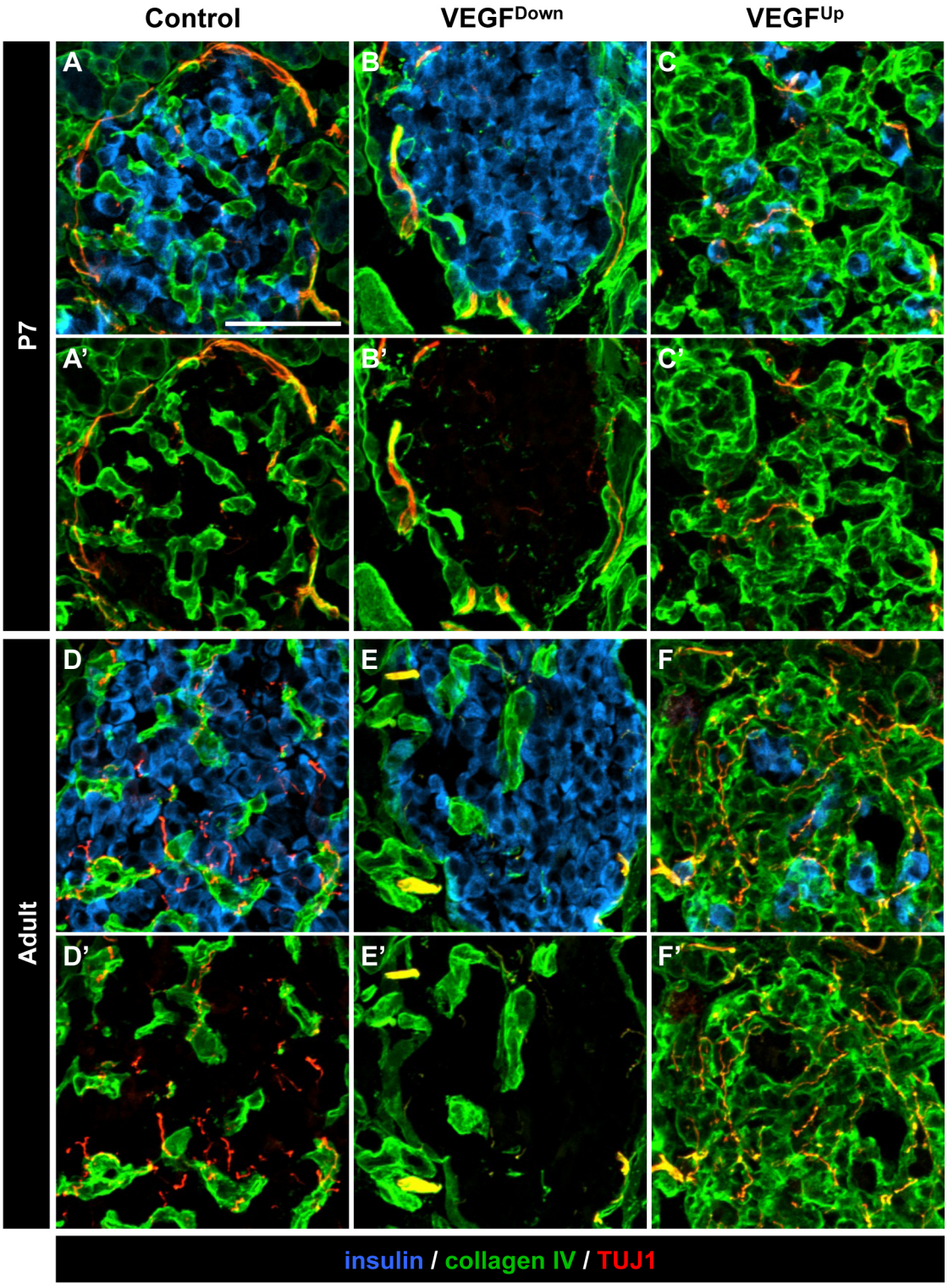

**Reinert Fig. S9**

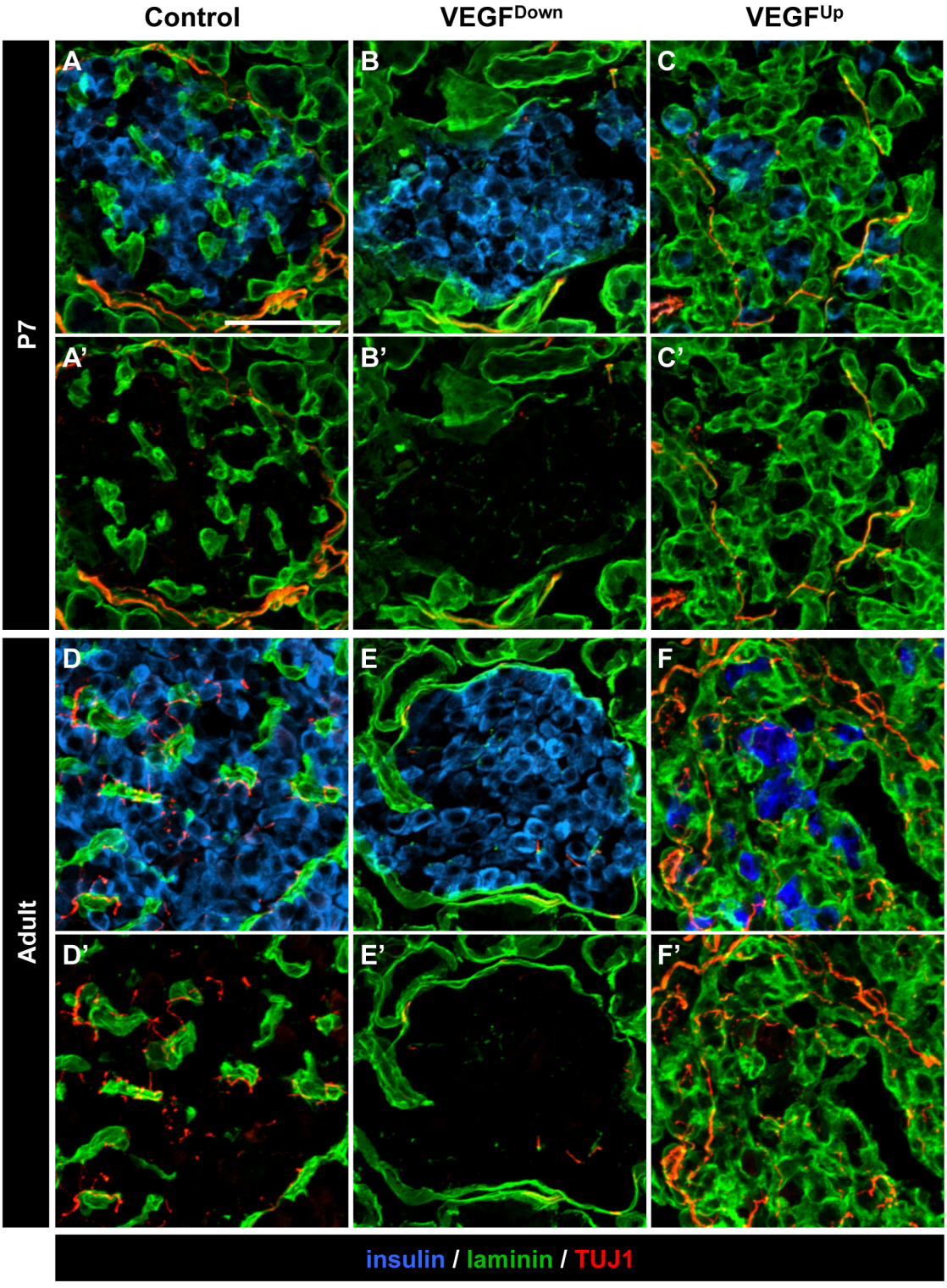

Reinert Fig. S10

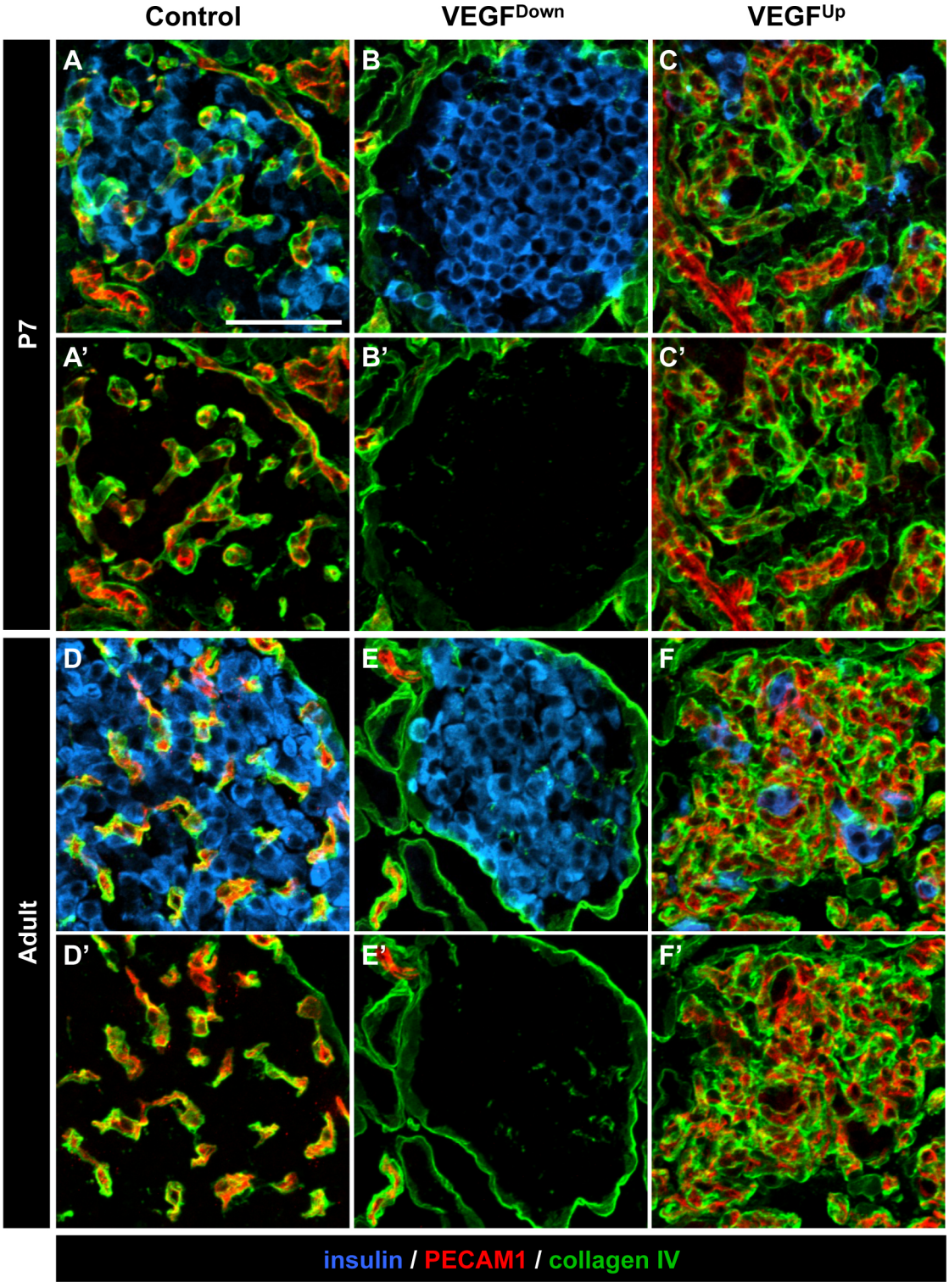

Reinert Fig. S11

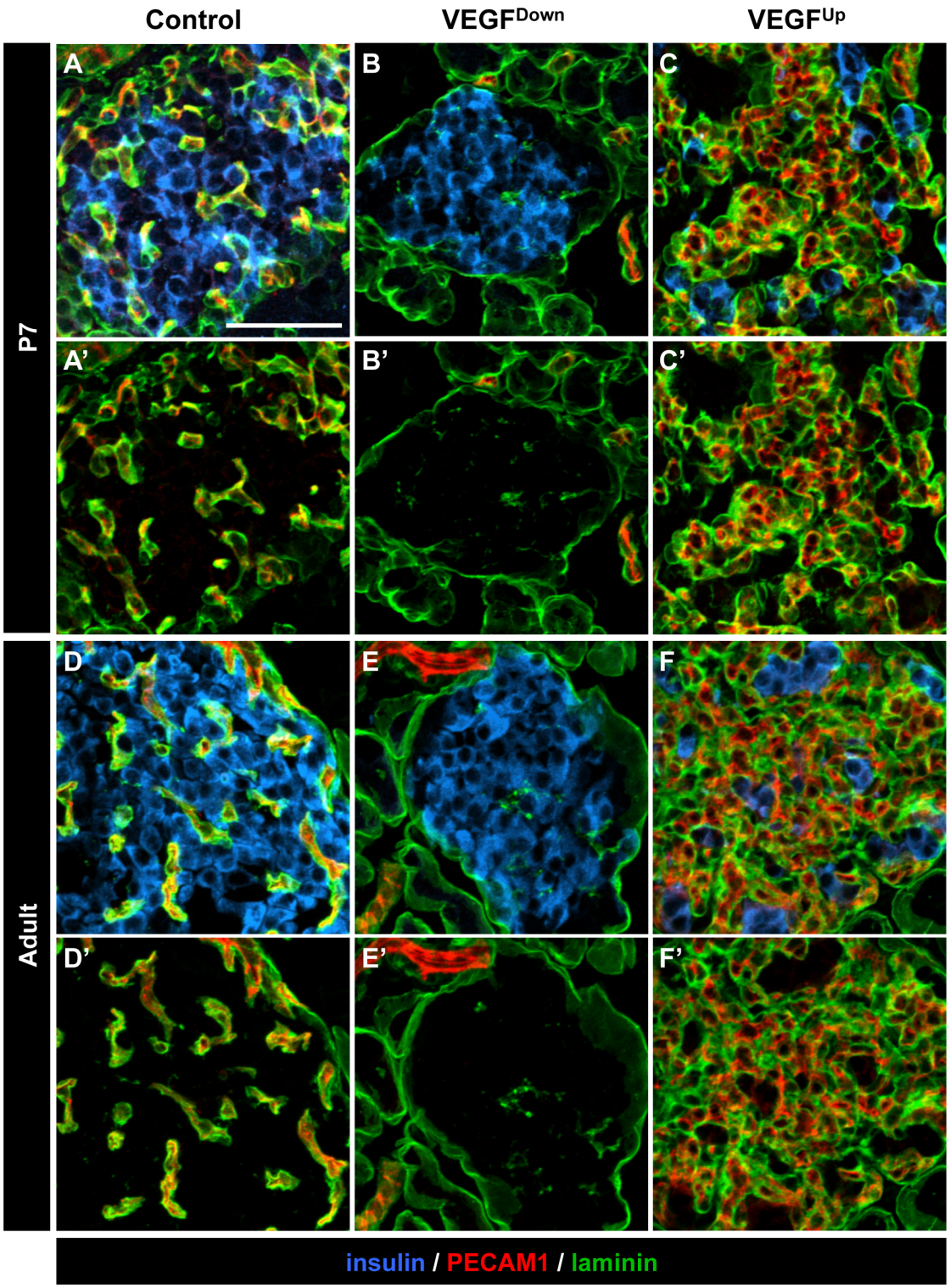

**SUPPLEMENTARY FIGURE LEGENDS**

**Fig. S1. Islet innervation follows islet VEGF production and vascularization. A**-**C**. Representative islets from adult control (**A**), *Pdx1-Cre;Vegfa*$^{fl/fl}$ (VEGF$^{Down}$; **B**), and doxycycline-treated (for one week) *RIP-rtTA;TetO-hVegfa* (VEGF$^{Up}$; **C**) mice, immunolabeled for insulin (blue), PECAM1 (green) and synapsin-1,-2 (red). Panels **A'**-**C'** show grayscale images of synapsin-1,-2 labeling in **A**-**C**. Regions denoted by the dashed line in **A**, **B**, and **C** are shown in **A''**, **B''** and **C''**, respectively. Closed arrowheads point to synapsin-1,-2+ neuronal structures in a complete or partial alignment with PECAM1+ capillaries. Open arrowheads designate synapsin-1,-2+ structures that were not adjacent to endothelial cells. Scale bars in **A**-**C** are 100 μm. Scale bars in **A''**-**C''** are 50 μm.

**Fig. S2. Pancreatic innervation during embryogenesis. A**-**D**. Images are 3D reconstructions of confocal z-stacks (30 μm-thick) of embryonic pancreata from control (**A, C**) and *Pdx1-Cre;Vegfa*$^{fl/fl}$ (VEGF$^{Down}$; **B, D**) mice at embryonic day 14.5 (E14.5; **A, B**) and E18.5 (**C, D**). Pancreata were immunolabeled in whole mount with antibodies to PDX1 (blue), PECAM1 (green), and TUJ1 (red). Scale bars in **A**-**D** are 100 μm, and correspond to all panels below.

**Fig. S3**. **Pancreatic vascularization is not altered by reduced innervation. A**, **B**. Images are 3D reconstructions of confocal z-stacks (15 μm-thick) of embryonic pancreata from *Foxd3*$^{fl/-}$ (**A**) and *Wnt1-Cre;Foxd3*$^{fl/-}$ (**B**) mice at embryonic day 16.5 (E16.5), immunolabeled in whole mount with antibodies to PDX1 (blue), PECAM1 (green), and TUJ1 (red). **A'**, **B'**. Grayscale images of PDX1 labeling from respective panels **A**, **B**. **A''**, **B''**. Grayscale images of PECAM1 labeling from respective panels **A**, **B**. **A'''**, **B'''**. Grayscale images of TUJ1 labeling from respective panels **A**, **B**. Scale bar in **A** is 50 μm, and corresponds to all other panels. **C**. Quantification of vessel density. Data are summarized as mean ± standard error of the mean (SEM).

**Fig. S4**. **Pancreatic islet innervation matures postnatally, and depends on VEGF expression.** Representative islets from control (**A**), *Pdx1-Cre;Vegfa*$^{fl/fl}$ (VEGF$^{Down}$; **B**), and doxycycline-treated (from E5.5) *RIP-rtTA;TetO-hVegfa* (VEGF$^{Up}$; **C**) mice at postnatal day 7 (P7). Pancreatic sections were immunolabeled for insulin (blue), PECAM1 (green) and TUJ1 (red/grayscale). Scale bars in **A**-**C** are 100 μm. Regions denoted by the dashed line in **A**-**C** are shown in **A'**-**C'**, respectively. Panels **A'**-**C'** show grayscale images of TUJ1 labeling in **A**-**C**. Scale bars in **A**'-**C**' are 50 μm.

**Fig. S5. The number of β-cells expressing tyrosine hydroxylase is elevated in VEGF-deficient islets during postnatal development. A**-**J**. Representative islets from *Vegfa*$^{fl/fl}$ (Control, **A**-**E**), *Pdx1-Cre;Vegfa*$^{fl/fl}$ (VEGF$^{Down}$; **F**-**J**), and doxycycline-treated (from embryonic day E5.5) *RIP-rtTA;TetO-hVegfa* (VEGF$^{Up}$; **K**) mice at E14.5 (**A, F**), E17.5 (**B**, **G**), postnatal day 1 (P1; **C, H**), P7 (**D, I, K**) and weaning (**E, J**), immunolabeled for insulin (green) and TH (red). Scale bars are 100 μm.

**Fig. S6. Islet neural crest-derived cells do not express VEGF receptors in postnatal life. A**-**C**. Representative islets from *Wnt1-Cre;R26-EYFP* mice at postnatal day 7 (P7; **A**), weaning (P21-P28; **B**), and adult (**C**) stages labeled for insulin (blue), GFP (green), and neuropilin 1 (NRP1, red). Regions denoted by the dotted line in **A'**, **B'**, and **C'** are shown in **A''**, **B''**, and **C''**, respectively. Scale bars in **A**-**C** are 100 μm. Scale bars in **A''**-**C''** are 50 μm. **D**-**F**. Representative islets from *Wnt1-Cre;R26-EYFP* mice at embryonic day 16.5 (E16.5; **D, F**) and postnatal day 1 (P1; **E**). Images are labeled for insulin (blue), GFP (green), and VEGFR2 (red in **D**-**E**) or neuropilin 1 (NRP1, red in **F**). Regions denoted by the dotted line in **D'**, **E'**, and **F'** are shown in **D''**, **E''** and **F'**, respectively. Arrowheads in **F** denote fibers with colocalization of GFP and NRP1. Scale bars in **D**-**F** are 100 μm. Scale bars in **D''**-**F''** are 50 μm.

**Fig. S7. Intraislet endothelial cells modulate islet innervation via synthesis of the vascular basement membrane. A**. Relative gene expression of *Ins2* (encoding insulin), *Pecam1* (encoding PECAM1), *Ngf*, (encoding nerve growth factor) *Col4a1* (encoding collagen IV α1), *Col4a2* (encoding collagen IV α2), *Itgb1* (encoding integrin β1), and *Lama4* (encoding laminin α4) in islets from doxycycline-treated (for one week) *RIP-rtTA;TetO-hVegfa* ($VEGF^{Up}$) mice compared to untreated *RIP-rtTA;TetO-hVegfa* controls, evaluated by quantitative RT-PCR. **B**. Relative gene expression of *Ins2*, *Kdr* (encoding VEGFR2), and *Ngf* in islets from *Pdx1-Cre;Vegfa*$^{fl/fl}$ ($VEGF^{Down}$) mice compared to *Vegfa*$^{fl/fl}$ controls, evaluated by quantitative RT-PCR. Data are summarized as mean ± standard error of the mean (SEM); $n = 4$; $^{**}P < 0.01$, $^{***}P < 0.001$.

**Fig. S8. Intraislet nerve fibers align with endothelial cells expressing collagen IV.** Representative islets from *Vegfa*$^{fl/fl}$ (Control, **A**, **D**), *Pdx1-Cre;Vegfa*$^{fl/fl}$ ($VEGF^{Down}$; **B, E**), and doxycycline-treated (from embryonic day E5.5) *RIP-rtTA;TetO-hVegfa* ($VEGF^{Up}$; **C, F**) mice at postnatal day 7 (P7; **A-C**) and adult (**D-F**) stages, immunolabeled for insulin (blue), collagen IV α1 (green) and TUJ1 (red). Images **A** and **D** are replicates of Fig. 7C-D. Panels **A'-F'** highlight collagen IV and TUJ1 labeling in islets from panels **A-F**. Scale bar in **A** is 50 μm and applies to all other panels.

**Fig. S9. Intraislet nerve fibers align with endothelial cells expressing laminin.** Representative islets from *Vegfa*$^{fl/fl}$ (Control, **A**, **D**), *Pdx1-Cre;Vegfa*$^{fl/fl}$ ($VEGF^{Down}$; **B, E**), and doxycycline-treated (from embryonic day E5.5) *RIP-rtTA;TetO-hVegfa* ($VEGF^{Up}$; **C, F**) mice at postnatal day 7 (P7; **A-C**) and adult (**D-F**) stages, immunolabeled for insulin (blue), laminin (green) and TUJ1 (red). Panels **A'-F'** highlight laminin and TUJ1 labeling in islets from panels **A-F**. Scale bar in **A** is 50 μm and applies to all other panels.

**Fig. S10. Endothelial cells produce collagen IV of the intraislet vascular basement membrane. A-F.** Representative islets from *Vegfa*$^{fl/fl}$ (Control, **A**, **D**), *Pdx1-Cre;Vegfa*$^{fl/fl}$ (VEGF$^{Down}$; **B, E**), and doxycycline-treated (from embryonic day E5.5) *RIP-rtTA;TetO-hVegfa* (VEGF$^{Up}$; **C, F**) mice at postnatal day 7 (P7; **A-C**) and adult (**D-F**) stages, immunolabeled for PECAM1 (red), and collagen IV α1 (green). Panels **A'-F'** highlight collagen IV and TUJ1 labeling in islets from panels **A-F**. In addition to the endothelial cell-associated collagen IV labeling, we noted some fine collagen IV+ fibers within VEGF$^{Down}$ islets; however, these fibers were rarely aligned with TUJ1+ nerve fibers. Scale bar in **A** is 50 μm and applies to all other panels.

**Fig. S11. Endothelial cells produce laminin of the intraislet vascular basement membrane. A-F.** Representative islets from *Vegfa*$^{fl/fl}$ (Control, **A**, **D**), *Pdx1-Cre;Vegfa*$^{fl/fl}$ (VEGF$^{Down}$; **B, E**), and doxycycline-treated (from embryonic day E5.5) *RIP-rtTA;TetO-hVegfa* (VEGF$^{Up}$; **C, F**) mice at postnatal day 7 (P7; **A-C**) and adult (**D-F**) stages, immunolabeled for PECAM1 (red) and laminin (green). Panels **A'-F'** highlight laminin and TUJ1 labeling in islets from panels **A-F**. In addition to the endothelial cell-associated laminin labeling, we noted some fine laminin+ fibers within VEGF$^{Down}$ islets; however, these fibers were rarely aligned with TUJ1+ nerve fibers. Scale bar in **A** is 50 μm and applies to all other panels.

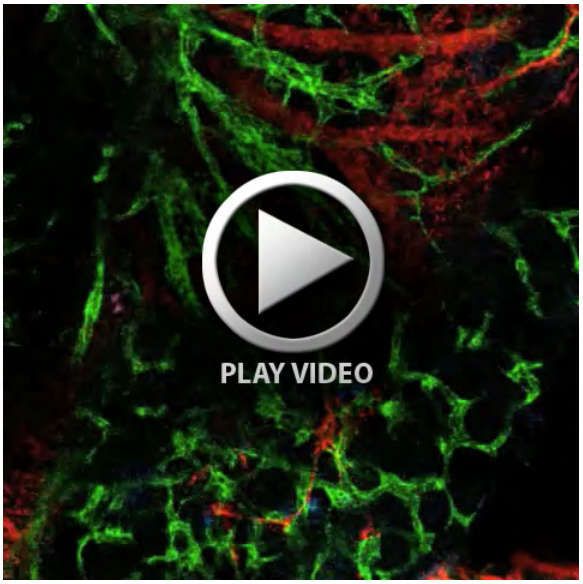


**Movie 1A.**

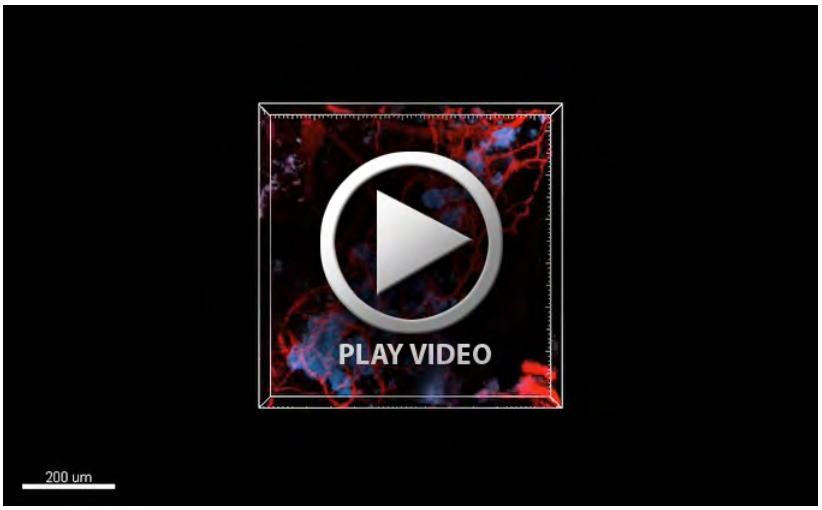


**Movie 1B.**

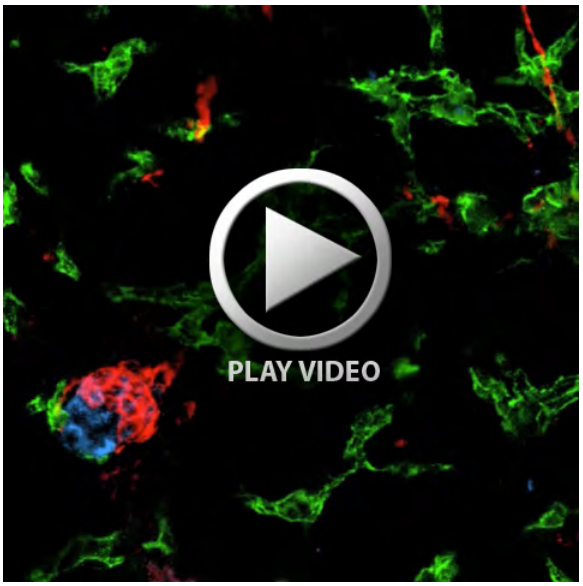


**Movie 2.**

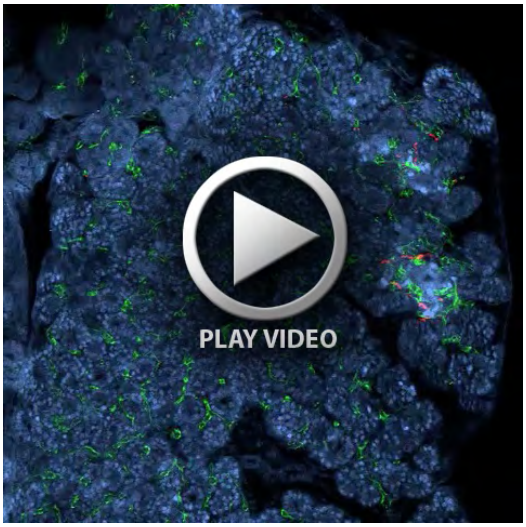


**Movie 3.**


**Movie 4.**

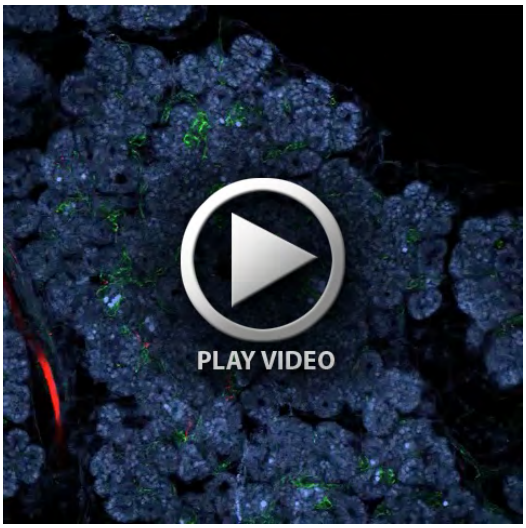


**Movie 5.**

**SUPPLEMENTARY MOVIE LEGENDS**

**Movie S1A. Developing pancreatic islets are interconnected by a network of nerves during embryogenesis.** Movie displays sequential confocal z-stack of a 100 μm-thick portion of pancreas from a control embryo at E14.5, immunolabeled in whole mount with antibodies to insulin and glucagon (blue), PECAM1 (green), and TUJ1 (red).

**Movie S1B. Three-D visualization of neuronal network interconnecting developing pancreatic islets.** Movie displays 3D reconstructed sequential confocal z-stack of a 100 μm-thick portion of pancreas from a control embryo at E14.5 (shown in Movie S1A), immunolabeled in whole mount with antibodies to insulin and glucagon (blue), and TUJ1 (red).

**Movie S2. Nerve processes are adjacent to, but do not expand, into developing pancreatic islets during embryogenesis.** Movie displays sequential confocal z-stack of a 67 μm-thick portion of pancreas from a control embryo at E14.5, immunolabeled in whole mount with antibodies to insulin and glucagon (blue), PECAM1 (green), and TUJ1 (red).

**Movie S3. The pancreas is well innervated in late embryogenesis.** Movie displays sequential confocal z-stack of a 30 μm-thick portion of pancreas from the control embryo shown in Fig. 4A. The pancreas was harvested at E16.5 and immunolabeled in whole mount with antibodies to PDX1 (blue), PECAM1 (green), and TUJ1 (red).

**Movie S4. VEGF is not required for pancreatic innervation during embryogenesis.** Movie displays sequential confocal z-stack of a 30 μm-thick portion of pancreas from the *Pdx1-Cre; Vegfa*$^{fl/fl}$ (VEGF$^{Down}$) embryo shown in Fig. 4B. The pancreas was harvested at E16.5 and immunolabeled in whole mount with antibodies to PDX1 (blue), PECAM1 (green), and TUJ1 (red).

**Movie S5. VEGF enhances pancreatic innervation during embryogenesis.** Movie displays sequential confocal z-stack of a 30 µm-thick portion of pancreas from the doxycycline-treated (from E5.5) *RIP-rtTA; TetO-hVegfa* ($VEGF^{Up}$) embryo shown in Fig. 4C. The pancreas was harvested at E16.5 and immunolabeled in whole mount with antibodies to PDX1 (blue), PECAM1 (green), and TUJ1 (red).

**SUPPLEMENTARY TABLES**

**Table S1. Sources and nomenclature of mouse strains used.**

| MGI Nomenclature | Abbreviation | Genotyping Primers | Reference |
|---|---|---|---|
| *Tg(Pdx1-cre)$^{89.1Dam}$* | *Pdx1-Cre* | 5'- TGC CAC GAC CAA GTG ACA GC -3'<br>5'- CCA GGT TAC GGA TAT AGT TCA TG -3' | Gu et al., 2002 |
| *Vegfa$^{tm2Gne}$* | *Vegfa$^{fl/fl}$* | 5'- CCT GGC CCT CAA GTA CAC CTT -3'<br>5'- TCC GTA CGA CGC ATT TCT AG -3' | Gerber et al., 1999 |
| *Tg(Ins2-rtTA)$^{2Efr}$* | *RIP-rtTA* | 5'- GTG AAG TGG GTC CGC GTA CAG -3'<br>5'- GTA CTC GTC AAT TCC AAG GGC ATC G -3' | Milo-Landesman et al., 2001 |
| Unlisted | *TetO-hVegfa* | 5'- TCG AGT AGG CGT GTA CGG -3'<br>5'- GCA GCA GCC CCC GCA TCG -3' | Ohno-Matsui et al., 2002 |
| *Tg(Wnt1-cre)$^{11Rth}$* | *Wnt1-Cre* | 5'- TGC CAC GAC CAA GTG ACA GC -3'<br>5'- CCA GGT TAC GGA TAT AGT TCA TG -3' | Danielian et al., 1998 |
| *Gt(ROSA)26Sor$^{tm1(EYFP)Cos}$* | *R26-EYFP* | 5'- GGA GCG GGA GAA ATG GAT ATG -3'<br>5'- AAA GTC GCT CTG AGT TGT TAT -3'<br>5'- AAG ACC GCG AAG AGT TTG TC -3' | Srinivas et al., 2001 |
| *Foxd3$^{tm1Lby}$, Foxd3$^{tm2Lby}$, Foxd3$^{tm3Lby}$* | *Foxd3$^{fl/-}$* | See Reference | Teng et al., 2008 |

**Table S2. Sources and concentrations of primary antibodies.**

| Antigen | Host Species | Working Dilutions | | Source | Catalog # |
|---|---|---|---|---|---|
| | | Cryo-sections | Whole Mount | | |
| **Collagen IV (alpha 1)** | rabbit | 1:1000 | - | Rockland | 600-401-106S |
| **Glucagon** | guinea pig | - | 1:10000 | Linco | 4031-01F |
| **Green Fluorescent Protein (GFP)** | chicken | 1:1000 | - | Abcam | ab13970 |
| **Insulin** | guinea pig | 1:200 | - | Linco | 4011-01F |
| **Insulin** | guinea pig | 1:500 | 1:500 | Dako | A0564 |
| **Laminin** | rabbit | 1:1000 | - | Sigma-Aldrich | L9393 |
| **Neuronal Class III β-Tubulin (TUJ1)** | rabbit | 1:20000 | 1:5000 | Covance | MRB-435P |
| **Neuropilin-1 (NRP1)** | rabbit | 1:50000 | - | Alex L. Kolodkin | (serum) |
| **PDX1** | goat | - | 1:5000 | C. V. E. Wright | (serum) |
| **mouse PECAM1 (a.k.a. CD31)** | rat | 1:50 | 1:100 | BD Pharmingen | 550274 |
| **proNGF** | rabbit | 1:1000 | - | Millipore | 04-1142 |
| **Synapsin-1, -2** | rabbit | 1:2000 | - | Synaptic Systems | 106 002 |
| **Tyrosine Hydroxylase (TH)** | rabbit | 1:1000 | - | Millipore | AB152 |
| **Vesicular Acetylcholine Transporter (VAChT)** | rabbit | 1:2000 | - | Synaptic Systems | 139 103 |
| **VEGFR2 (a.k.a. FLK1, KDR)** | rabbit | 1:2000 | - | Rolf Brekken | T014 |

**Table S3. Sources and concentrations of secondary antibodies.**

| Host Species | Primary Ab Species | Fluorophore | Working Dilutions | | Vendor | Catalog # |
|---|---|---|---|---|---|---|
| | | | Cryosections | Whole Mount | | |
| donkey | rabbit | Cy2 | 1:200 | 1:200 | Jackson Labs | 711-225-152 |
| donkey | | Cy3 | 1:500 | 1:500 | Jackson Labs | 711-165-152 |
| donkey | | Cy5 | 1:200 | 1:500 | Jackson Labs | 711-175-152 |
| donkey | goat | Cy3 | - | 1:500 | Jackson Labs | 705-165-147 |
| donkey | rat | Cy2 | 1:200 | 1:200 | Jackson Labs | 712-225-153 |
| donkey | | DyLight649 | - | 1:500 | Jackson Labs | 712-495-153 |
| donkey | chicken | Cy2 | 1:200 | - | Jackson Labs | 703-225-155 |
| donkey | | Cy3 | 1:500 | - | Jackson Labs | 703-165-155 |
| donkey | guinea pig | Cy2 | 1:200 | - | Jackson Labs | 706-225-148 |
| donkey | | Cy3 | 1:500 | - | Jackson Labs | 706-165-148 |
| donkey | | Cy5 | 1:200 | 1:500 | Jackson Labs | 706-175-148 |

**Table S4. Primers for quantitative real-time RT-PCR.**

| Gene Symbol | TaqMan Assay ID |
|---|---|
| *Gfap* | Mm01253033_m1 |
| *Ins2* | Mm00731595_gh |
| *Kdr* | Mm00440099_m1 |
| *Ngf* | Mm00443039_m1 |
| *Pecam1* | Mm01242584_m1 |
| *Col4a1* | Mm01210125_m1 |
| *Col4a2* | Mm00802386_m1 |
| *Fn1* | Mm01256744_m1 |
| *Itgb1* | Mm01253230_m1 |
| *Lama4* | Mm01193660_m1 |
| *Tbp* | Mm00446973_m1 |

**Table S5. Gene expression of axon guidance molecules, extracellular matrix components, and neurotrophic growth factors in VEGF$^{Up}$ islets.** RNA sequencing was performed on control and VEGF$^{Up}$ islets, and sorted endothelial cells isolated from VEGF$^{Up}$ islets.

| | Gene Symbol | Normalized Expression Whole Islets, Control | Normalized Expression Whole Islets, VEGFUp | LOG2 of Fold Change Whole Islets VEGFUp vs. Control | Normalized Expression Islet Endothelial Cells, VEGFUp |
|---|---|---|---|---|---|
| Netrins and Slits | Ntn1 | 69 +/- 24 | 88 +/- 27 | 0.35408 | 68 +/- 14 |
| | Ntn3 | 28 +/- 11 | 10 +/- 3 | -1.54535 | 15 +/- 2 |
| | Ntn4 | 841 +/- 75 | 981 +/- 229 | 0.22124 | 1654 +/- 194 |
| | Ntn5 | 1 +/- 0 | 1 +/- 0 | -0.27269 | 1 +/- 0 |
| | Ntng1 | 44 +/- 18 | 17 +/- 7 | -1.34627 | 1 +/- 0 |
| | Ntng1 | 1 +/- 0 | 1 +/- 0 | 0.00000 | 1 +/- 0 |
| | Ntng2 | 92 +/- 54 | 153 +/- 67 | 0.73513 | 232 +/- 14 |
| | Slit1 | 7 +/- 5 | 4 +/- 2 | -0.88264 | 13 +/- 4 |
| | Slit2 | 641 +/- 89 | 806 +/- 130 | 0.33001 | 23 +/- 15 |
| | Slit3 | 1796 +/- 201 | 4308 +/- 357 | 1.26195 | 2604 +/- 70 |
| | Slitrk1 | 31 +/- 10 | 6 +/- 1 | -2.25950 | 1 +/- 0 |
| | Slitrk2 | 50 +/- 9 | 66 +/- 17 | 0.39838 | 27 +/- 13 |
| | Slitrk3 | 85 +/- 27 | 19 +/- 6 | -2.15752 | 2 +/- 1 |
| | Slitrk4 | 2 +/- 1 | 1 +/- 0 | -0.63164 | 2 +/- 1 |
| | Slitrk5 | 8 +/- 6 | 2 +/- 1 | -2.13142 | 1 +/- 0 |
| | Slitrk6 | 9967 +/- 3269 | 3710 +/- 1049 | -1.42580 | 8 +/- 3 |
| Semaphorins | Sema3a | 20 +/- 5 | 24 +/- 11 | 0.22995 | 41 +/- 4 |
| | Sema3b | 60 +/- 20 | 92 +/- 10 | 0.60942 | 22 +/- 3 |
| | Sema3c | 431 +/- 55 | 403 +/- 64 | -0.09921 | 166 +/- 32 |
| | Sema3d | 28 +/- 6 | 82 +/- 11 | 1.53649 | 104 +/- 22 |
| | Sema3e | 277 +/- 69 | 178 +/- 35 | -0.63679 | 1 +/- 0 |
| | Sema3f | 450 +/- 236 | 1542 +/- 812 | 1.77555 | 4398 +/- 497 |
| | Sema3g | 478 +/- 96 | 939 +/- 206 | 0.97260 | 1297 +/- 30 |
| | Sema4a | 230 +/- 51 | 184 +/- 34 | -0.32395 | 57 +/- 10 |
| | Sema4b | 415 +/- 147 | 293 +/- 116 | -0.50192 | 95 +/- 7 |
| | Sema4c | 146 +/- 85 | 181 +/- 90 | 0.30460 | 718 +/- 41 |
| | Sema4d | 786 +/- 129 | 523 +/- 37 | -0.58743 | 29 +/- 5 |
| | Sema4f | 211 +/- 19 | 164 +/- 40 | -0.36329 | 2 +/- 1 |
| | Sema4g | 71 +/- 24 | 52 +/- 29 | -0.43122 | 24 +/- 6 |
| | Sema5a | 6544 +/- 2339 | 13444 +/- 3054 | 1.03870 | 6914 +/- 1094 |
| | Sema5b | 105 +/- 17 | 484 +/- 31 | 2.19858 | 155 +/- 9 |
| | Sema6a | 2271 +/- 749 | 4206 +/- 195 | 0.88882 | 12941 +/- 539 |
| | Sema6b | 205 +/- 76 | 252 +/- 82 | 0.29934 | 1195 +/- 32 |
| | Sema6c | 11 +/- 8 | 12 +/- 8 | 0.03231 | 16 +/- 2 |
| | Sema6d | 6321 +/- 412 | 22593 +/- 3080 | 1.83759 | 42069 +/- 3396 |
| | Sema7a | 579 +/- 118 | 1277 +/- 392 | 1.14122 | 3185 +/- 543 |
| Ephrins | Efna1 | 151 +/- 42 | 477 +/- 121 | 1.66064 | 1337 +/- 99 |
| | Efna2 | 26 +/- 6 | 17 +/- 8 | -0.62701 | 5 +/- 2 |
| | Efna3 | 1 +/- 0 | 3 +/- 1 | 1.19947 | 7 +/- 1 |
| | Efna4 | 8 +/- 3 | 15 +/- 12 | 0.82975 | 41 +/- 11 |
| | Efna5 | 1915 +/- 571 | 607 +/- 87 | -1.65696 | 36 +/- 9 |
| | Efnb1 | 79 +/- 38 | 78 +/- 17 | -0.02113 | 154 +/- 26 |
| | Efnb2 | 3474 +/- 280 | 10546 +/- 1411 | 1.60227 | 18080 +/- 629 |
| | Efnb3 | 82 +/- 6 | 68 +/- 8 | -0.25838 | 81 +/- 10 |
| Morphogens | Shh | 1 +/- 0 | 1 +/- 0 | 0.00000 | 2 +/- 1 |
| | Wnt1 | 1 +/- 0 | 1 +/- 0 | 0.00000 | 1 +/- 0 |
| | Wnt2 | 1 +/- 0 | 1 +/- 0 | 0.00000 | 1 +/- 0 |
| | Wnt2b | 834 +/- 162 | 561 +/- 54 | -0.57272 | 605 +/- 24 |
| | Wnt3 | 3 +/- 1 | 3 +/- 2 | 0.03665 | 1 +/- 0 |
| | Wnt3a | 1 +/- 0 | 1 +/- 0 | 0.00000 | 1 +/- 0 |
| | Wnt4 | 1428 +/- 108 | 1062 +/- 69 | -0.42715 | 32 +/- 4 |
| | Wnt5a | 161 +/- 6 | 131 +/- 29 | -0.29360 | 8 +/- 1 |
| | Wnt5b | 141 +/- 31 | 106 +/- 29 | -0.41064 | 42 +/- 5 |
| | Wnt6 | 11 +/- 5 | 1 +/- 0 | -3.40839 | 1 +/- 0 |
| | Wnt7a | 1 +/- 0 | 1 +/- 0 | -0.15040 | 1 +/- 0 |
| | Wnt7b | 1 +/- 0 | 1 +/- 0 | 0.32828 | 1 +/- 0 |
| | Wnt8a | 1 +/- 0 | 1 +/- 0 | 0.17691 | 2 +/- 0 |
| | Wnt8b | 3 +/- 2 | 4 +/- 1 | 0.30619 | 5 +/- 1 |
| | Wnt9a | 11 +/- 5 | 36 +/- 13 | 1.66513 | 12 +/- 4 |
| | Wnt9b | 1 +/- 0 | 1 +/- 0 | 0.00000 | 3 +/- 1 |
| | Wnt10a | 1 +/- 0 | 2 +/- 1 | 0.69369 | 1 +/- 0 |
| | Wnt10b | 1 +/- 0 | 1 +/- 0 | 0.00000 | 1 +/- 0 |
| | Wnt11 | 4 +/- 2 | 3 +/- 1 | -0.59459 | 2 +/- 1 |
| | Wnt16 | 86 +/- 16 | 46 +/- 15 | -0.89629 | 141 +/- 18 |

**Table S5, continued.**

| | | | | | |
|---|---|---|---|---|---|
| **Cell adhesion** | | | | | |
| | Dscam | 367 +/- 229 | 123 +/- 39 | -1.57419 | 5 +/- 3 |
| | Cdh2 | 7111 +/- 1359 | 4006 +/- 627 | -0.82778 | 185 +/- 88 |
| | Cdh5 | 3507 +/- 141 | 12840 +/- 1543 | 1.87231 | 36807 +/- 1690 |
| **Extracellular Matrix Components** | | | | | |
| | Col1a1 | 1958 +/- 384 | 8808 +/- 1337 | 2.16981 | 134 +/- 35 |
| | Col1a2 | 5513 +/- 1159 | 25269 +/- 5023 | 2.19645 | 1033 +/- 458 |
| | Col2a1 | 1 +/- 0 | 1 +/- 0 | 0.00000 | 2 +/- 1 |
| | Col3a1 | 13058 +/- 5126 | 37177 +/- 11062 | 1.50943 | 883 +/- 337 |
| | Col4a1 | 11583 +/- 2448 | 67236 +/- 8402 | 2.53727 | 99045 +/- 2187 |
| | Col4a2 | 6154 +/- 817 | 34632 +/- 2807 | 2.49239 | 47663 +/- 2104 |
| | Col4a3 | 1829 +/- 469 | 3403 +/- 790 | 0.89602 | 3100 +/- 302 |
| | Col4a4 | 1237 +/- 383 | 1755 +/- 195 | 0.50386 | 735 +/- 76 |
| | Col4a5 | 190 +/- 25 | 875 +/- 94 | 2.20173 | 50 +/- 12 |
| | Col4a6 | 43 +/- 9 | 146 +/- 51 | 1.75969 | 18 +/- 3 |
| | Col5a1 | 270 +/- 31 | 1304 +/- 227 | 2.27224 | 35 +/- 11 |
| | Col5a2 | 1259 +/- 387 | 4705 +/- 698 | 1.90149 | 486 +/- 45 |
| | Col5a3 | 82 +/- 27 | 285 +/- 96 | 1.79232 | 25 +/- 7 |
| | Col6a1 | 579 +/- 70 | 2617 +/- 251 | 2.17663 | 137 +/- 72 |
| | Col6a2 | 944 +/- 15 | 3473 +/- 361 | 1.87899 | 217 +/- 91 |
| | Col6a3 | 884 +/- 82 | 4476 +/- 500 | 2.34000 | 136 +/- 41 |
| | Col6a4 | 2 +/- 1 | 10 +/- 5 | 2.16337 | 1 +/- 0 |
| | Col6a5 | 131 +/- 41 | 50 +/- 9 | -1.40495 | 4 +/- 3 |
| | Col6a6 | 2367 +/- 172 | 963 +/- 103 | -1.29774 | 179 +/- 29 |
| | Col7a1 | 9 +/- 5 | 21 +/- 9 | 1.22448 | 18 +/- 1 |
| | Col8a1 | 1102 +/- 369 | 5775 +/- 2012 | 2.38941 | 160 +/- 18 |
| | Col8a2 | 17 +/- 5 | 7 +/- 5 | -1.33111 | 2 +/- 1 |
| | Col9a1 | 2 +/- 1 | 1 +/- 0 | -0.69061 | 1 +/- 0 |
| | Col9a2 | 5 +/- 2 | 2 +/- 1 | -1.00842 | 3 +/- 1 |
| | Col9a3 | 18 +/- 11 | 12 +/- 3 | -0.51717 | 26 +/- 7 |
| | Col10a1 | 55 +/- 16 | 600 +/- 127 | 3.45101 | 106 +/- 8 |
| | Col11a1 | 30 +/- 7 | 157 +/- 28 | 2.38079 | 1 +/- 0 |
| | Col11a2 | 29 +/- 7 | 18 +/- 7 | -0.64115 | 26 +/- 10 |
| | Col12a1 | 240 +/- 12 | 1577 +/- 219 | 2.71414 | 349 +/- 107 |
| | Col13a1 | 1440 +/- 426 | 2968 +/- 243 | 1.04357 | 8492 +/- 649 |
| | Col14a1 | 1002 +/- 11 | 1664 +/- 198 | 0.73113 | 49 +/- 3 |
| | Col15a1 | 2835 +/- 275 | 13363 +/- 2767 | 2.23712 | 24391 +/- 512 |
| | Col16a1 | 38 +/- 4 | 95 +/- 7 | 1.32947 | 14 +/- 8 |
| | Col17a1 | 46 +/- 17 | 64 +/- 30 | 0.48413 | 90 +/- 20 |
| | Col18a1 | 265 +/- 76 | 2108 +/- 603 | 2.99237 | 3069 +/- 390 |
| | Col19a1 | 243 +/- 63 | 995 +/- 257 | 2.03323 | 129 +/- 35 |
| | Col20a1 | 226 +/- 78 | 138 +/- 8 | -0.70603 | 174 +/- 16 |
| | Col22a1 | 876 +/- 101 | 627 +/- 55 | -0.48361 | 588 +/- 28 |
| | Col23a1 | 22 +/- 12 | 34 +/- 8 | 0.62666 | 95 +/- 15 |
| | Col24a1 | 3 +/- 2 | 21 +/- 7 | 2.86652 | 5 +/- 4 |
| | Col25a1 | 534 +/- 319 | 397 +/- 62 | -0.42801 | 1716 +/- 320 |
| | Col27a1 | 444 +/- 97 | 399 +/- 30 | -0.15489 | 54 +/- 28 |
| | Col28a1 | 554 +/- 132 | 567 +/- 189 | 0.03458 | 203 +/- 10 |
| | Fn1 | 532 +/- 93 | 6499 +/- 926 | 3.60996 | 508 +/- 44 |
| | Lama1 | 2 +/- 1 | 8 +/- 1 | 1.82105 | 2 +/- 1 |
| | Lama2 | 2826 +/- 538 | 5958 +/- 415 | 1.07601 | 424 +/- 169 |
| | Lama3 | 3369 +/- 1314 | 4940 +/- 544 | 0.55228 | 19154 +/- 696 |
| | Lama4 | 3205 +/- 415 | 16453 +/- 2689 | 2.35973 | 41212 +/- 1162 |
| | Lama5 | 639 +/- 217 | 1839 +/- 725 | 1.52610 | 6219 +/- 251 |
| | Lamb1 | 2700 +/- 479 | 13567 +/- 1955 | 2.32933 | 30771 +/- 2041 |
| | Lamb2 | 618 +/- 253 | 1599 +/- 553 | 1.37196 | 2530 +/- 87 |
| | Lamb3 | 9 +/- 6 | 11 +/- 3 | 0.27096 | 2 +/- 0 |
| | Lamc1 | 7231 +/- 503 | 34826 +/- 5211 | 2.26785 | 74832 +/- 2396 |
| | Lamc2 | 405 +/- 77 | 178 +/- 16 | -1.18803 | 34 +/- 5 |
| | Lamc3 | 129 +/- 39 | 194 +/- 14 | 0.59111 | 33 +/- 15 |

**Table S5, continued.**

| | | | | | |
|---|---|---|---|---|---|
| Integrins | Itga1 | 8509 +/- 2067 | 23945 +/- 3901 | 1.49274 | 19757 +/- 1358 |
| | Itga2 | 537 +/- 137 | 1164 +/- 239 | 1.11503 | 1839 +/- 87 |
| | Itga2b | 36 +/- 17 | 26 +/- 13 | -0.49847 | 47 +/- 6 |
| | Itga3 | 757 +/- 164 | 908 +/- 121 | 0.26330 | 2536 +/- 121 |
| | Itga4 | 2630 +/- 823 | 2966 +/- 333 | 0.17327 | 354 +/- 46 |
| | Itga5 | 407 +/- 71 | 2404 +/- 451 | 2.56390 | 5556 +/- 330 |
| | Itga6 | 4787 +/- 456 | 15533 +/- 2536 | 1.69814 | 30155 +/- 903 |
| | Itga7 | 390 +/- 148 | 955 +/- 303 | 1.29065 | 137 +/- 64 |
| | Itga8 | 329 +/- 99 | 1253 +/- 200 | 1.92972 | 73 +/- 34 |
| | Itga9 | 732 +/- 32 | 2663 +/- 117 | 1.86402 | 3554 +/- 304 |
| | Itga10 | 86 +/- 33 | 224 +/- 120 | 1.37727 | 180 +/- 13 |
| | Itga11 | 70 +/- 11 | 91 +/- 15 | 0.37742 | 9 +/- 2 |
| | Itgad | 867 +/- 260 | 40 +/- 17 | -4.45208 | 1 +/- 0 |
| | Itgae | 53 +/- 19 | 77 +/- 12 | 0.54989 | 62 +/- 4 |
| | Itgal | 93 +/- 22 | 233 +/- 54 | 1.32527 | 20 +/- 11 |
| | Itgam | 216 +/- 45 | 645 +/- 104 | 1.57494 | 7 +/- 3 |
| | Itgav | 8029 +/- 754 | 8048 +/- 410 | 0.00331 | 5705 +/- 206 |
| | Itgax | 213 +/- 35 | 384 +/- 107 | 0.85331 | 5 +/- 1 |
| | Itgb1 | 4894 +/- 430 | 15747 +/- 1913 | 1.68588 | 14708 +/- 213 |
| | Itgb2 | 188 +/- 30 | 398 +/- 40 | 1.08008 | 12 +/- 9 |
| | Itgb2l | 9 +/- 5 | 6 +/- 2 | -0.77748 | 1 +/- 0 |
| | Itgb3 | 660 +/- 79 | 3230 +/- 333 | 2.29223 | 5007 +/- 444 |
| | Itgb4 | 152 +/- 43 | 192 +/- 26 | 0.33247 | 473 +/- 60 |
| | Itgb5 | 832 +/- 194 | 1510 +/- 302 | 0.85938 | 1206 +/- 113 |
| | Itgb6 | 49 +/- 22 | 50 +/- 7 | 0.03110 | 46 +/- 18 |
| | Itgb7 | 111 +/- 24 | 70 +/- 25 | -0.66228 | 118 +/- 20 |
| | Itgb8 | 1497 +/- 161 | 884 +/- 101 | -0.76016 | 16 +/- 7 |
| | Itgbl1 | 577 +/- 93 | 642 +/- 136 | 0.15519 | 9 +/- 6 |
| Neurotrophic Growth Factors | Artn | 5 +/- 2 | 6 +/- 3 | 0.15315 | 1 +/- 0 |
| | Bdnf | 107 +/- 51 | 306 +/- 32 | 1.51836 | 26 +/- 14 |
| | Bmp1 | 1159 +/- 471 | 1351 +/- 489 | 0.22088 | 2061 +/- 255 |
| | Bmp2 | 108 +/- 28 | 299 +/- 39 | 1.47398 | 208 +/- 10 |
| | Bmp3 | 425 +/- 151 | 312 +/- 154 | -0.44671 | 10 +/- 9 |
| | Bmp4 | 192 +/- 18 | 232 +/- 65 | 0.26969 | 124 +/- 6 |
| | Bmp5 | 351 +/- 162 | 709 +/- 142 | 1.01341 | 97 +/- 48 |
| | Bmp6 | 330 +/- 42 | 351 +/- 46 | 0.08585 | 925 +/- 101 |
| | Bmp7 | 8 +/- 2 | 40 +/- 22 | 2.32573 | 3 +/- 2 |
| | Bmp8a | 1 +/- 0 | 1 +/- 0 | 0.53337 | 4 +/- 2 |
| | Bmp8b | 13 +/- 5 | 9 +/- 5 | -0.53416 | 8 +/- 1 |
| | Bmp10 | 8 +/- 4 | 11 +/- 0 | 0.47941 | 40 +/- 4 |
| | Bmp15 | 6 +/- 2 | 19 +/- 3 | 1.58359 | 38 +/- 13 |
| | Edn1 | 99 +/- 17 | 178 +/- 30 | 0.84897 | 502 +/- 61 |
| | Edn2 | 2 +/- 1 | 2 +/- 1 | 0.11662 | 1 +/- 0 |
| | Edn3 | 249 +/- 41 | 88 +/- 10 | -1.50214 | 2 +/- 1 |
| | Gdnf | 6 +/- 5 | 24 +/- 2 | 1.89393 | 2 +/- 1 |
| | Hgf | 340 +/- 101 | 416 +/- 99 | 0.29307 | 20 +/- 8 |
| | Ngf | 866 +/- 324 | 1302 +/- 224 | 0.58877 | 123 +/- 63 |
| | Ntf3 | 89 +/- 34 | 30 +/- 16 | -1.54684 | 32 +/- 2 |
| | Ntf5 | 1 +/- 0 | 1 +/- 0 | -0.25374 | 1 +/- 0 |